Chapter 5

PYRRHOTITE REACTIVITY

5.1 Introduction

As described in Chapter 2, pyrrhotite is a highly reactive sulfide mineral that is prone to oxidation. Severe oxidation of pyrrhotite and subsequent formation of hydrophilic iron hydroxides will have a detrimental effect on flotation performance. Since the accounts in the literature with respect to the role of mineralogy on pyrrhotite oxidation are in conflict (Section 2.3.3), it is necessary to characterise the differences in the reactivity of magnetic and non-magnetic pyrrhotite on a set of pyrrhotite samples for which the mineralogy is already well-known (Chapter 4). Therefore the aim of this chapter is to "*explore and compare the reactivity of magnetic and non-magnetic pyrrhotite*". In order to do this, a series of electrochemical measurements comprising open circuit potential and cyclic voltammetry, as well as determination of the oxygen uptake of a pyrrhotite slurry have been performed; the results of which are presented in this chapter. Due to the nature of the experiments, reactivity measurements were only performed on the high grade pyrrhotite samples: Nkomati mixed pyrrhotite, Phoenix magnetic pyrrhotite, Sudbury CCN non-magnetic pyrrhotite and Sudbury Gertrude West magnetic pyrrhotite. The complete set of results from this chapter is presented in Appendix B.

5.2 Open Circuit Potential

Open circuit or rest potential measurements were used to investigate differences in surface oxidation between the different mineral electrodes. The open circuit potential describes the mixed potential between the anodic oxidation of pyrrhotite and the cathodic reduction of oxygen at the surface of pyrrhotite. Since the oxidation rate is influenced by the presence of the hydroxide species, it is expected that differences will be observed for different pH conditions (Section 2.3.3) and different ore samples. Results of the open circuit potential measurements for the Nkomati MSB mixed pyrrhotite, Phoenix magnetic pyrrhotite, Sudbury CCN non-magnetic pyrrhotite and Sudbury Gertrude West magnetic pyrrhotite samples are shown at pH 7 and pH 10 in figures 5.1 and 5.2, respectively.

5.2.1 Comparison of the Open Circuit Potentials of Pyrrhotite Samples

The open circuit potential of the Sudbury CCN non-magnetic pyrrhotite was the highest (170 mV) of the pyrrhotite samples investigated at pH 7 (Figure 5.1). Sudbury Gertrude West magnetic pyrrhotite and Nkomati MSB mixed pyrrhotite had slightly lower and similar open circuit potentials (~ 140 mV). The open circuit potential of the Phoenix magnetic pyrrhotite was the lowest at pH 7 (117 mV). The results at pH 10 were quite different to pH 7, possibly due to differences in rates of electrochemical reactions at the different pH values. At pH 10, the open circuit potential of Gertrude West magnetic pyrrhotite (116 mV) was significantly greater than the other pyrrhotite samples for which the open circuit potential was less than 44 mV (Figure 5.2). The lowest open circuit potential measurement was obtained for Sudbury CCN non-magnetic pyrrhotite (15 mV).

Since the differences between the open circuit potential measurements of the different electrodes at pH 7 were not as significant as they were at pH 10, it is under these conditions that any inferences relating to differences in pyrrhotite reactivity are drawn. Consequently, it can be inferred that at pH 10, the Sudbury Gertrude West pyrrhotite sample was the most oxidised and had the greatest proportion of ferric hydroxide species on the electrode surface in comparison to the other pyrrhotite samples. In contrast, the Sudbury CCN non-magnetic pyrrhotite sample was the least oxidised as evidenced by the very low open circuit potential obtained at pH 10 (15 mV; Figure 5.2).

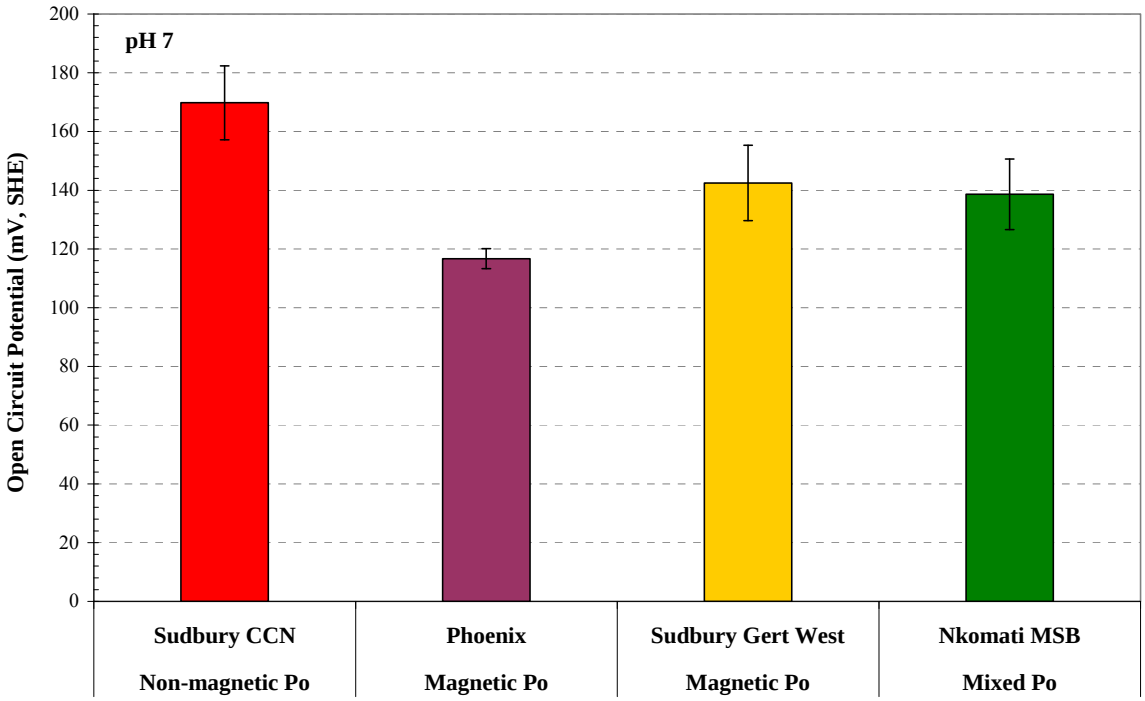

Figure 5.1: Open circuit potential for pyrrhotite samples at pH 7. The 2σ standard deviation is also shown.

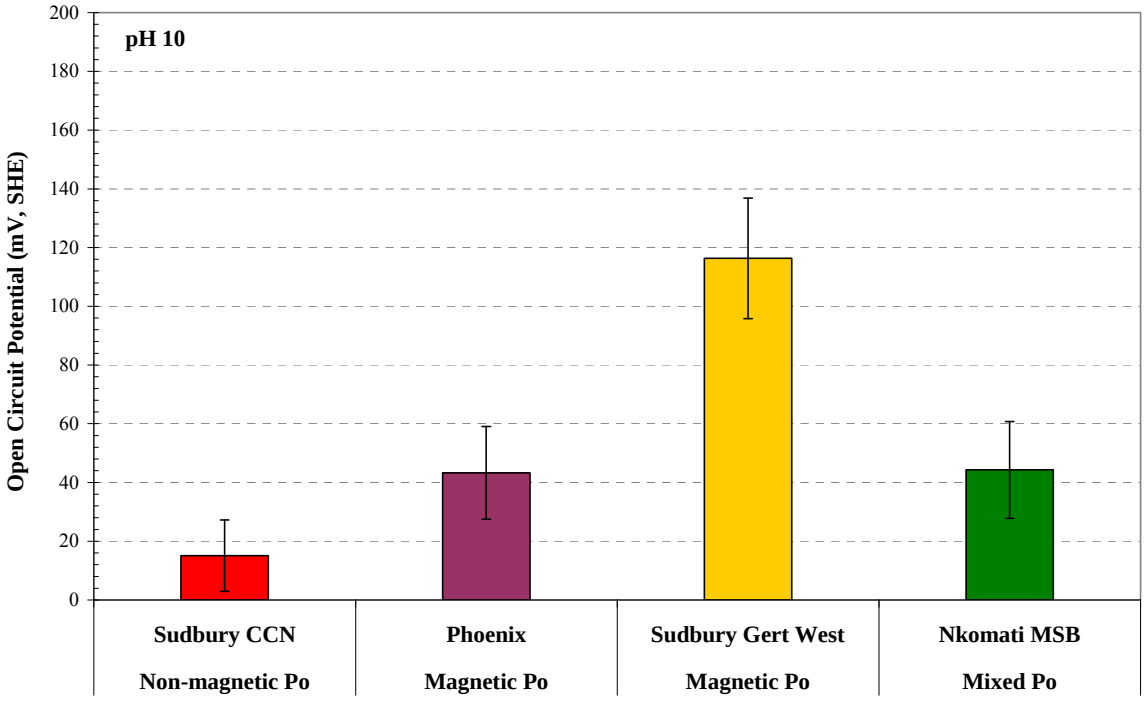

Figure 5.2: Open circuit potential for pyrrhotite samples at pH 10. The 2σ standard deviation is also shown.

5.3 Cyclic Voltammetry

Cyclic voltammetry was used to investigate differences in the surface reactions of the different pyrrhotite samples by varying the potential of the pyrrhotite electrode through several anodic and cathodic sweeps. Cyclic voltammetry was performed on electrodes of the Nkomati MSB mixed pyrrhotite, Phoenix magnetic pyrrhotite, Sudbury CCN non-magnetic pyrrhotite and Sudbury Gertrude West magnetic pyrrhotite at both pH 7 and 10. The cyclic voltammograms showed similar shapes to those obtained in other studies of pyrrhotite that were accounted for by typical pyrrhotite REDOX reactions found in the literature (e.g. Hamilton and Woods, 1984; Buswell and Nicol, 2002) and similar to those given in Section 2.3.1.

5.3.1 Nkomati MSB Pyrrhotite

The cyclic voltammogram of Nkomati MSB mixed pyrrhotite at pH 7 in figure 5.3 shows that for the first two sweeps from -800 to -300 mV, and -800 to -100 mV, there were no significant anodic or cathodic peaks. Only when the potential was increased to + 100 mV for the third scan, was an anodic peak at ~ 100 mV recognised (A1). A second anodic peak formed only when the potential was further increased from + 500 to + 700 mV, and which is annotated as A2 in figure 5.3. Three cathodic peaks were recognised and which were the most well developed for the scan from – 800 to + 700 mV, at ~ -100 mV (C1), ~ -300 (C2) and ~ -500 mV (C3), respectively. For the potential sweep from -800 to +700 mV, the maximum anodic current density achieved for reaction A1 was 34 $\mu A.cm^{-2}$, and a maximum cathodic current density of - 48 $\mu A.cm^{-2}$ for reaction C3.

Similarly to the results obtained at pH 7, the first anodic peak A1 was recognised on the potential sweep at pH 10 from -800 to +100 mV, followed by a second anodic peak A2 as shown in figure 5.4. On the return scan from the -800 to + 300 mV sweep, the cathodic peaks C1 and C2 were recognised at ~ -300 and -500 mV, respectively. In addition, a third anodic peak was recognised at ~ -200 mV when the upper limit of the sweep was increased to +500 mV. For the potential sweep from -800 to +700 mV, the maximum current density achieved for reaction A1 was 78 $\mu A.cm^{-2}$, and a maximum cathodic current density of -125 $\mu A.cm^{-2}$ for reaction C2.

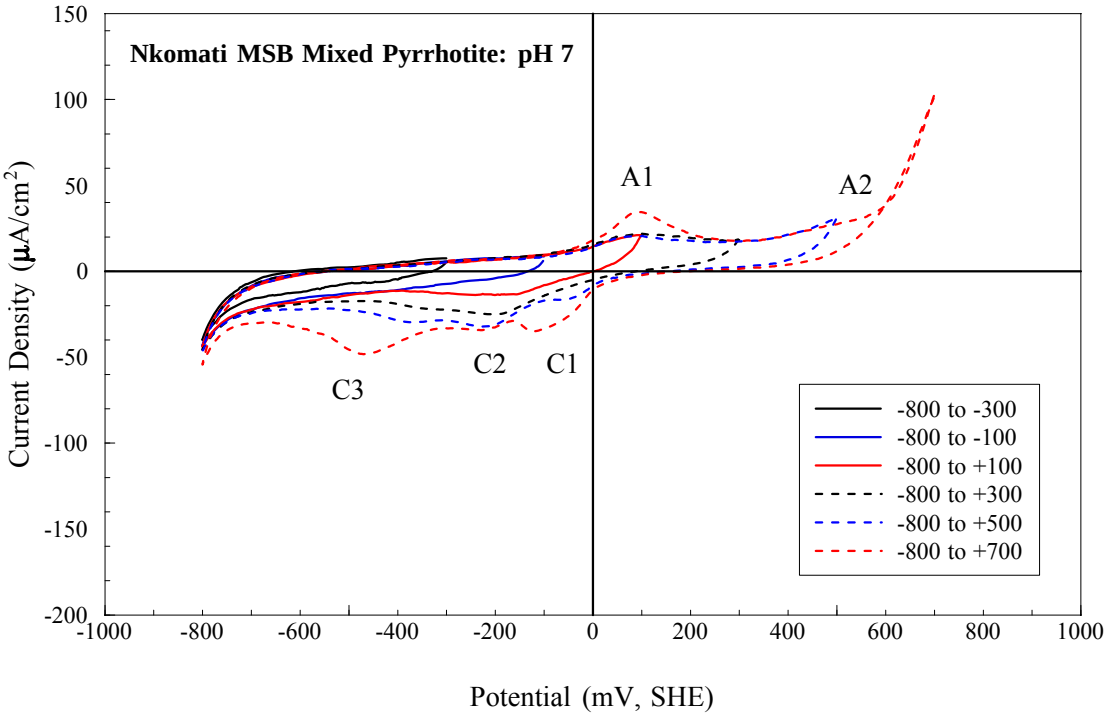

Figure 5.3: Cyclic voltammogram of Nkomati MSB mixed pyrrhotite at pH 7 for different anodic switching potentials.

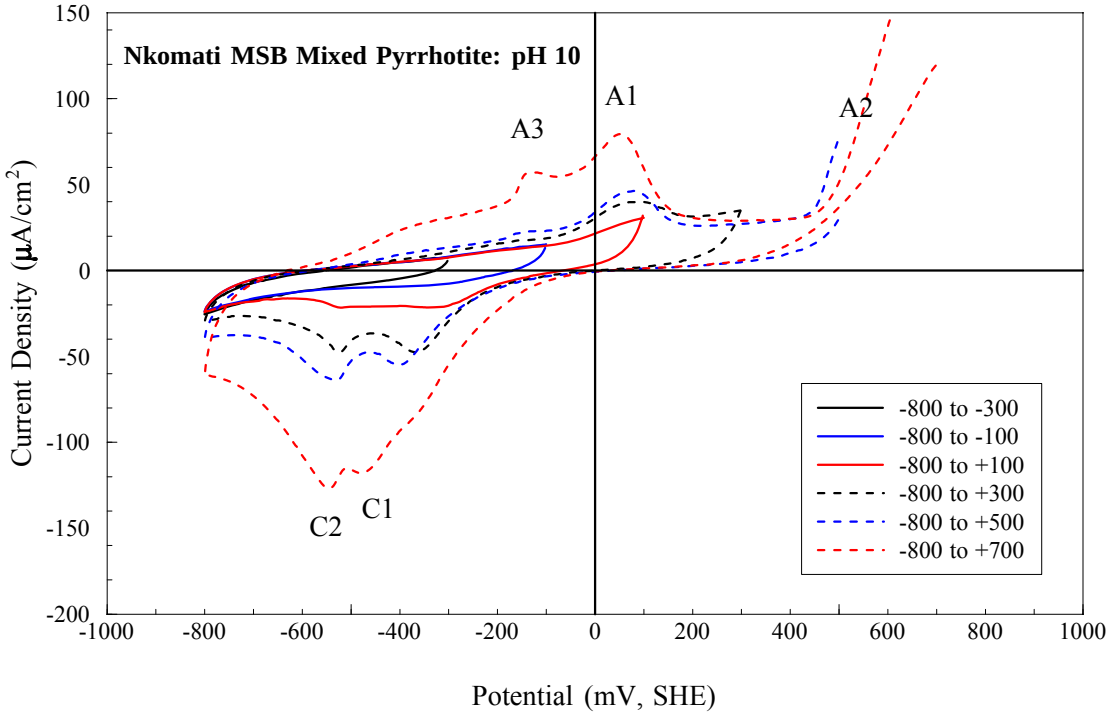

Figure 5.4: Cyclic voltammogram of Nkomati MSB mixed pyrrhotite at pH 10 for different anodic switching potentials.

5.3.2 Phoenix Pyrrhotite

Similarly to the behaviour of the Nkomati MSB mixed pyrrhotite electrode at pH 7, the Phoenix magnetic pyrrhotite showed an anodic reaction A1 when the upper limit of the potential sweep was increased to +100 mV as shown in figure 5.5. The corresponding cathodic reaction C1 was noted at ~ -100 mV. At greater positive potentials, a second anodic peak was recognised at ~ 600 mV. The cathodic reactions C2 and C3 were also noted at ~ -300 and - 500 mV, respectively.

The effect of an increase in pH from 7 to 10 as shown in figures 5.5 and 5.6, respectively, was to influence the reaction rates. For the anodic reaction A1 at pH 7, the maximum current density obtained for the Phoenix magnetic pyrrhotite was 53 $\mu A.cm^{-2}$, whereas at pH 10 the current density increased to 110 $\mu A.cm^{-2}$. A third anodic reaction A3 was also noted at ~ -200 mV when the upper limit of the potential was further increased. The cathodic reactions C1 and C2 were particularly prominent for the largest potential sweeps (-800 to + 700 mV) where the current density reached a maximum cathodic current density of almost - 200 $\mu A.cm^{-2}$.

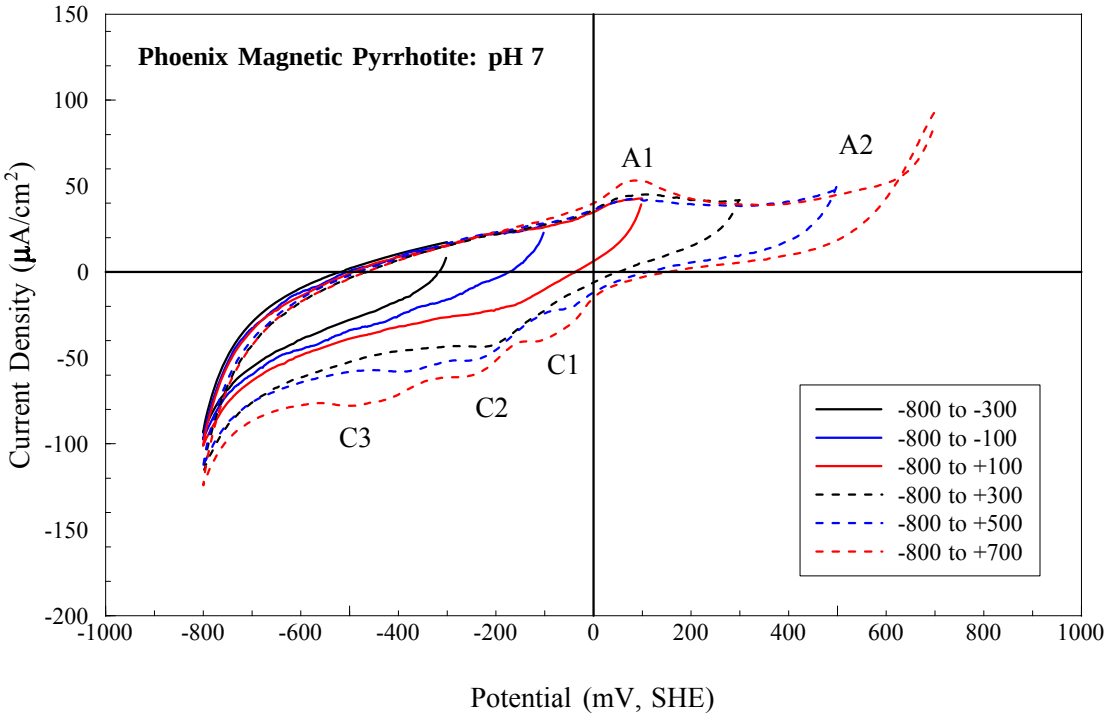

Figure 5.5: Cyclic voltammogram of Phoenix magnetic pyrrhotite at pH 7 for different anodic switching potentials.

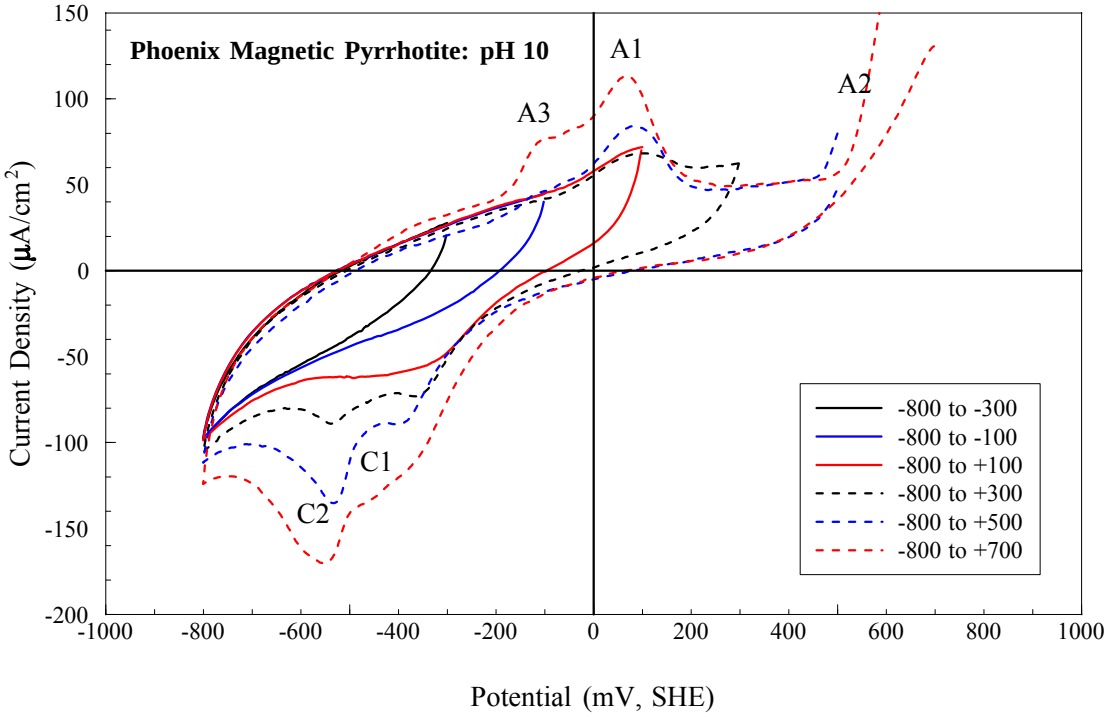

Figure 5.6: Cyclic voltammogram of Phoenix magnetic pyrrhotite at pH 10 for different anodic switching potentials.

5.3.3 Sudbury CCN Pyrrhotite

It is notable that the current density for all anodic and cathodic cycles was relatively small in the cyclic voltammetry studies of the Sudbury CCN non-magnetic pyrrhotite at pH 7 and pH 10 (Figures 5.7, 5.8). This suggests that the Sudbury CCN non-magnetic pyrrhotite was not particularly reactive towards oxidation and reduction even when the potential was increased to very oxidising conditions (> + 500 mV). However, similarly to the cyclic voltammograms from the Nkomati and Phoenix pyrrhotite electrodes, two anodic (A1, A2) and three cathodic (C1, C2, C3) peaks were recognised at pH 7.

The cyclic voltammogram for Sudbury CCN at pH 10 shown in figure 5.8 however, only shows two anodic peaks, A1 and A2. Even when the upper limit of the potential for the sweep was increased to + 700 mV, no additional anodic peaks were recognised. Two minor cathodic peaks C1 and C2 were recognised at ~ -300 and -500 mV, respectively.

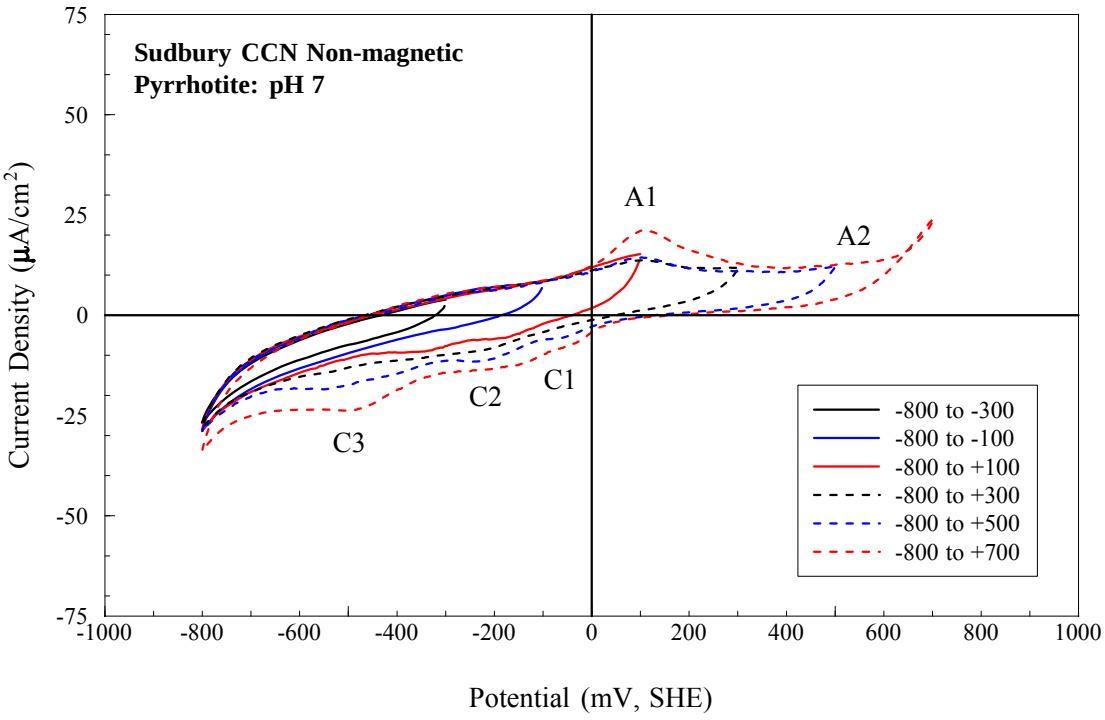

Figure 5.7: Cyclic voltammogram of Sudbury CCN non-magnetic pyrrhotite at pH 7 for different anodic switching potentials.

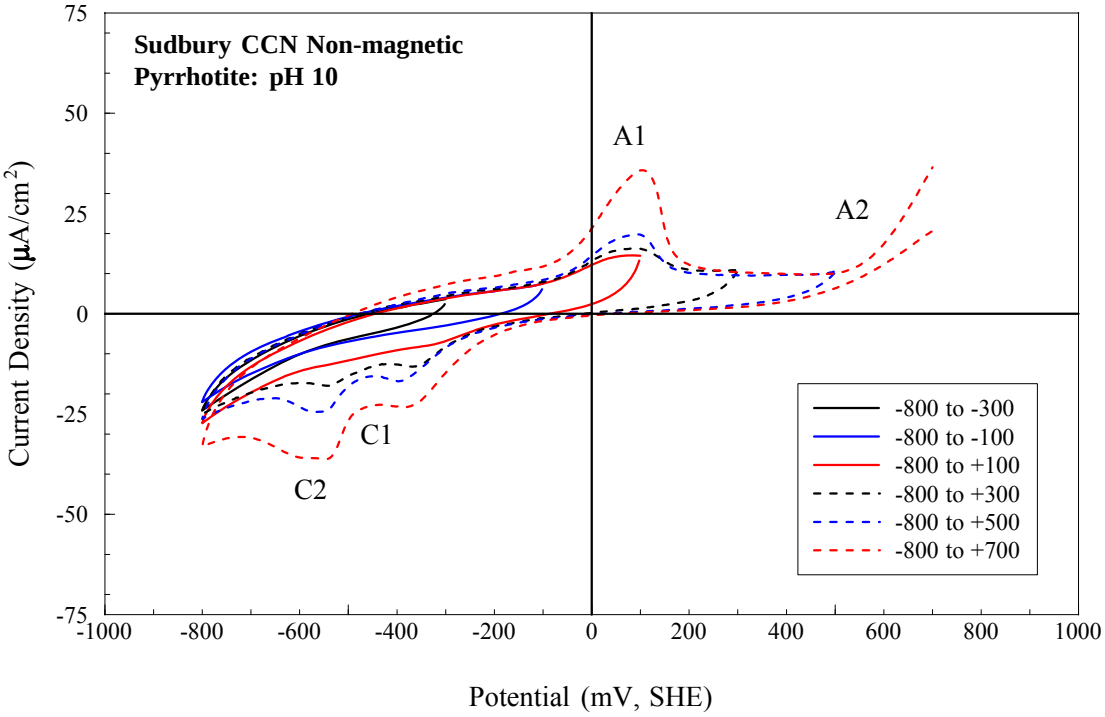

Figure 5.8: Cyclic voltammogram of Sudbury CCN non-magnetic pyrrhotite at pH 10 for different anodic switching potentials.

5.3.4 Sudbury Gertrude West Pyrrhotite

The cyclic voltammograms for the Sudbury Gertrude West magnetic pyrrhotite shown in figures 5.9 and 5.10 for pH 7 and 10, respectively, show well developed anodic and cathodic peaks. This is due to the intensity of the current associated with the electrochemical reactions that took place at the surface of the Gertrude West pyrrhotite electrode. At pH 7, two anodic peaks (A1, A2) and three cathodic peaks (C1, C2, C3) were recognised. For the potential sweeps associated with the most oxidising potentials, the current density associated with reaction A2 exceeded 75 $\mu A.cm^{-2}$. The current density associated with the most intense cathodic reaction C3, was less than -100 $\mu A.cm^{-2}$.

The current density associated with these electrochemical reactions was even more intense at pH 10 for the Sudbury Gertrude West magnetic pyrrhotite as shown in figure 5.10. Similarly to the Phoenix and Nkomati pyrrhotite samples, three anodic peaks (A1, A2 and A3) and two cathodic peaks (C2, C2) were recognised. For the potential sweeps associated with the most oxidising potentials, the current density associated with reaction A2 exceeded 250 $\mu A.cm^{-2}$. The current density associated with the most intense cathodic reaction C2, was less than -200 $\mu A.cm^{-2}$.

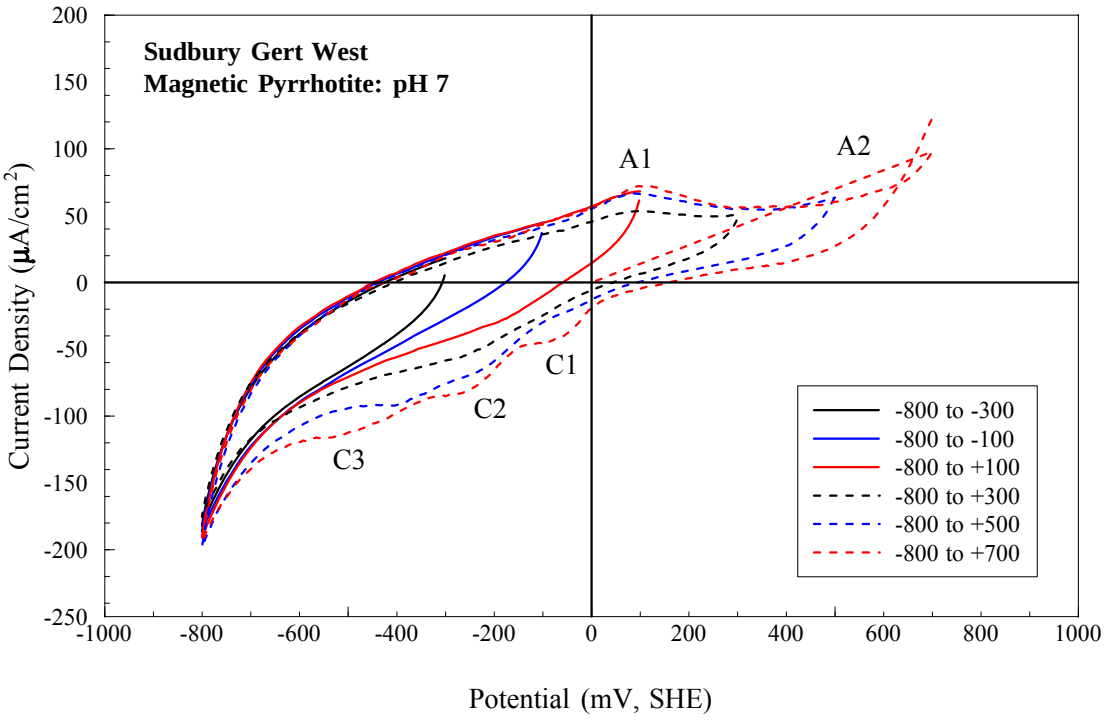

Figure 5.9: Cyclic voltammogram of Sudbury Gertrude West magnetic pyrrhotite at pH 7 for different anodic switching potentials.

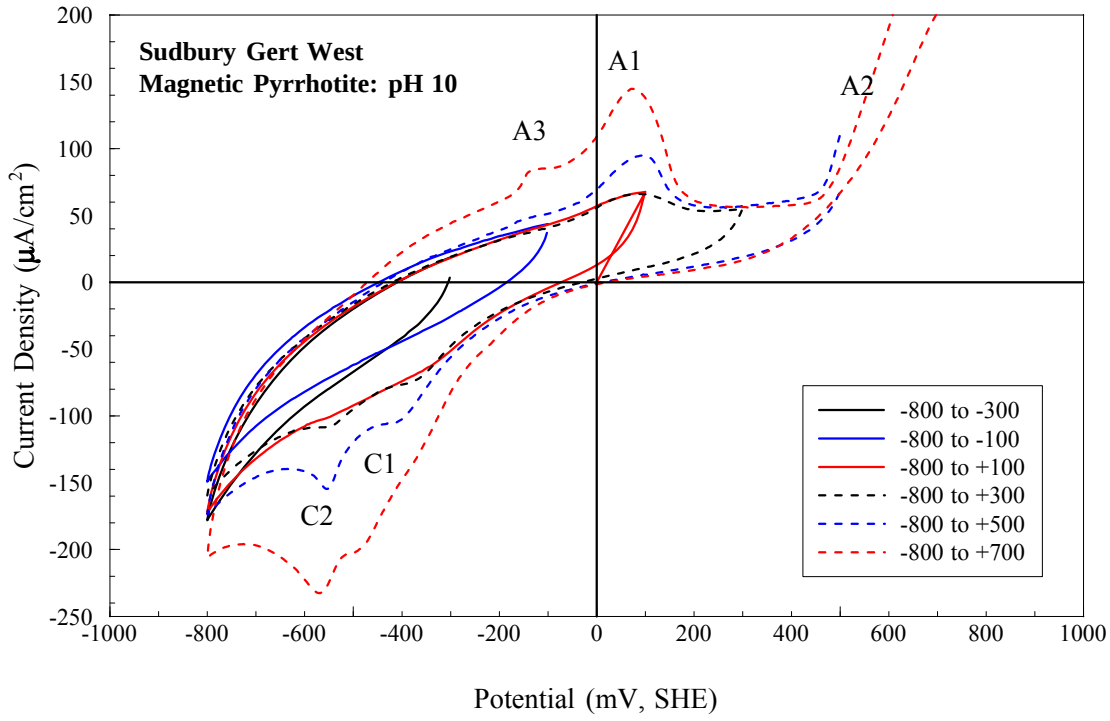

Figure 5.10: Cyclic voltammogram of Sudbury Gertrude West magnetic pyrrhotite at pH 10 for different anodic switching potentials.

5.3.5 Comparison of the Cyclic Voltammetry of Pyrrhotite Samples

In order to compare the reactivity of the different pyrrhotite samples, the cyclic voltammogram obtained for each pyrrhotite sample corresponding to the sweep from -800 to +700mV is shown in figures 5.11 and 5.12 for pH 7 and 10, respectively. Comparison of the voltammograms for the pyrrhotite samples examined at pH 7 shows that each of the pyrrhotite samples showed two anodic and three cathodic peaks at similar potentials. In general, the current density was greater at the higher pH due to the increase in reaction rates associated with the increase in hydroxide ion concentration. At pH 10, it is also evident that the Nkomati mixed pyrrhotite, Phoenix magnetic pyrrhotite and Sudbury Gertrude West magnetic pyrrhottie electrodes showed three anodic peaks whereas Sudbury CCN non-magnetic pyrrhotite only showed two. The anodic reaction A3 did not occur for the Sudbury CCN non-magnetic pyrrhotite at pH 10, which could be directly related to differences in pyrrhotite reactivity.

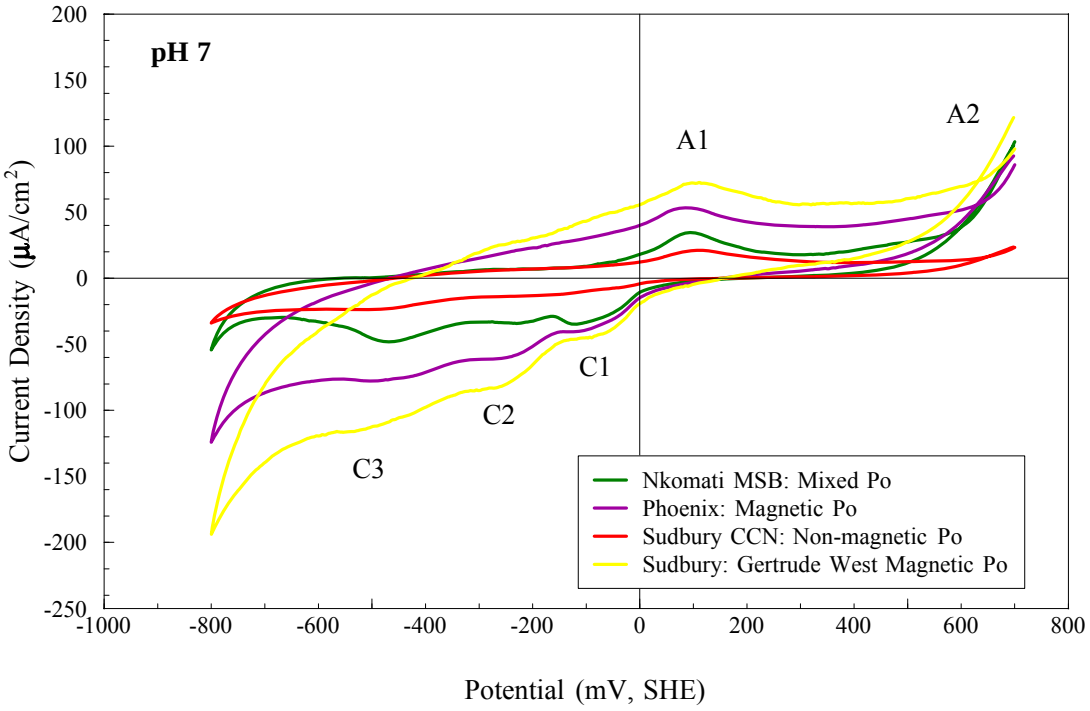

Figure 5.11: Comparison of the cyclic voltammograms obtained for the different pyrrhotite samples at pH 7 for the sweep from -800 to +700 mV.

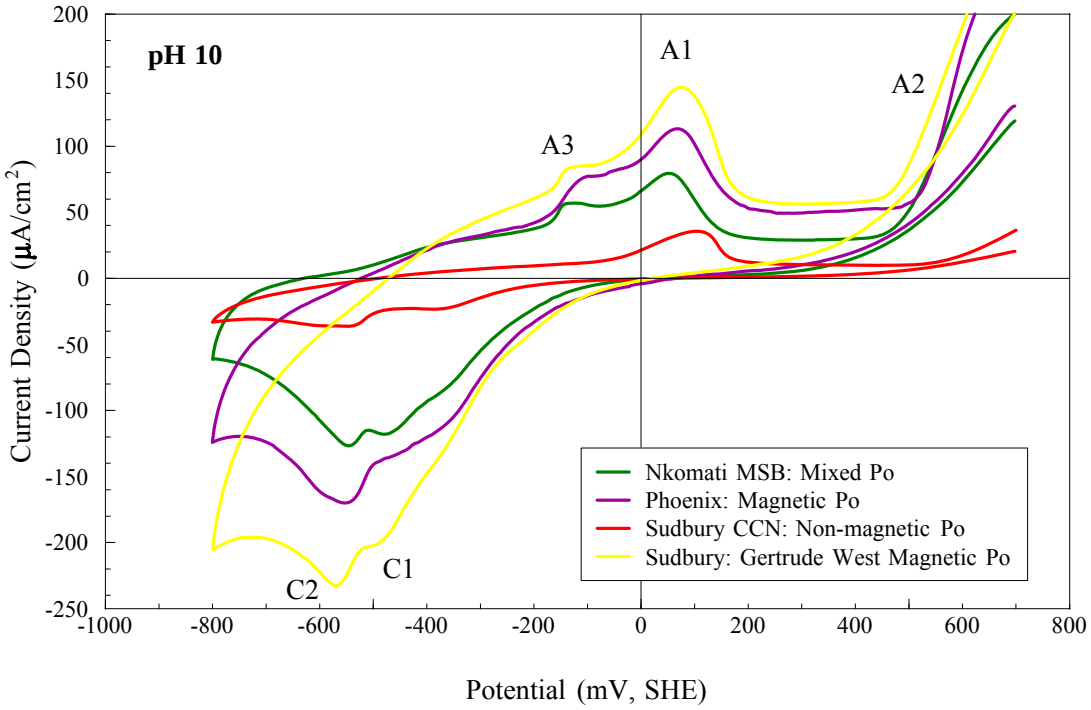

Figure 5.12: Comparison of the cyclic voltammograms obtained for the different pyrrhotite samples at pH 10 for the sweep from -800 to +700 mV.

The most prominent difference in the cyclic voltammograms for the different pyrrhotites is the large differences in current density which were correlated with the extent of the reactions. These can be directly related to the varying reactivity of the different pyrrhotite samples. Since the lowest current density occurred for Sudbury CCN non-magnetic pyrrhotite, it is indicative that it had the lowest reactivity of the samples examined. The current density for Nkomati mixed pyrrhotite was slightly larger and therefore the pyrrhotite was a little more reactive. The two magnetic pyrrhotite samples showed the greatest changes in current density and suggests that they were the most reactive. Magnetic Sudbury Gertrude West pyrrhotite however, showed the greatest changes in current density, and therefore the fastest reaction rates which indicates that it was the most reactive towards oxidation and reduction of the samples examined in this study.

5.4 Oxygen Uptake

Previous authors such as Spira and Rosenblum (1974), Greet and Brown (2000) and Johnson and Munro (2008) have recognised the significance of the oxygen demand of pyrrhotite rich ores in flotation. Consequently, a series of reactivity tests were performed to determine the oxygen uptake of the pyrrhotite samples investigated in this study. The tests were designed to measure the amount of dissolved oxygen in a slurry consumed through pyrrhotite oxidation. The tests were designed to simulate the conditions observed in the microflotation tests so that the results are comparable (Section 3.4, 3.5). Three sets of reagent conditions were explored, that consisted of no collector addition (collectorless), collector addition and collector plus activator addition, where copper sulfate was used for activation. Two collectors, namely SNPX and the longer chain length SIBX were used. The tests were carried out at pH 7 and pH 10. The mineralogical composition of the samples used is given in tables 3.1 and 3.3. Once the individual samples were suitably conditioned with reagents and the pH set to the desired pH, the mineral slurry was sparged with pure oxygen for a set time and then the decay of dissolved oxygen in the pyrrhotite slurry was measured. An exponential curve was fitted to the graph comparing the change in dissolved oxygen with time, and the coefficient of the slope of the curve used as the dissolved oxygen uptake factor. Table 5.1 summarises the calculated oxygen uptake factors obtained for the various pyrrhotite samples. An example of the calculation of the oxygen uptake factor, repeatability of the measurement and the raw data are given in Appendix B.

Table 5.1: Summary of oxygen uptake factors obtained in pyrrhotite reactivity tests for the various pyrrhotite samples. The associated R^2 is also given for the calculated oxygen uptake factor.

Pyrrhotite		**Nkomati MSB** Mixed		**Phoenix** Magnetic		**Sudbury CCN** Non-magnetic		**Sudbury Gert West** Magnetic	
Conditions	**pH**	Factor	R^2	Factor	R^2	Factor	R^2	Factor	R^2
Collectorless	7	15	0.998	29	0.997	9	0.999	17	0.998
SNPX	7	14	0.997	24	0.997	12	0.997	14	0.992
SNPX + Cu	7	-	-	16	0.991	-	-	8	0.983
SIBX	7	14	0.998	28	0.999	7	0.974	12	0.983
SIBX + Cu	7	18	0.998	16	0.997	12	0.997	9	0.982
Collectorless	10	60	0.998	110	0.995	8	0.999	36	0.995
SNPX	10	25	0.999	60	0.999	6	0.997	33	0.999
SNPX + Cu	10	-	-	28	0.995	2	0.981	14	0.998
SIBX	10	24	0.997	49	0.998	6	0.996	29	0.994
SIBX + Cu	10	17	0.999	31	0.999	10	0.999	13	0.998

5.4.1 Nkomati MSB Pyrrhotite

Following the conditioning of the Nkomati MSB mixed magnetic and non-magnetic pyrrhotite slurry with reagents, the pH was approximately neutral prior to pH modification for the associated mineral reactivity tests. The dissolved oxygen content of the mineral slurry after modification to pH 7 and prior to oxygen sparging varied between 2.3 and 5.7 ppm as shown in figure 5.13. The variability in initial dissolved oxygen content was likely a function of the conditioning procedure for each of the different tests given that different reagents were added for the various tests (SIBX, SNPX, Cu), each with their own respective conditioning times. Following sparging, the dissolved oxygen content of the slurry showed a progressive increase up to a maximum of 8.4 ppm for the SNPX test, 8.9 ppm for the collectorless test, 10.4 ppm for the SIBX test and up to 11.9 ppm for the SIBX with copper test. Once the maximum dissolved oxygen content had been reached, the dissolved oxygen levels showed a distinct decrease with time. The calculated oxygen uptake factors given in table 5.1 however, showed little difference between the different tests at pH 7. The highest factor was obtained for the SIBX with copper test (O_2 Uptake factor = 18) and the lowest for the SIBX and SNPX tests (O_2 Uptake factor = 14).

The dissolved oxygen contents of the slurry at pH 10 prior to sparging with oxygen were generally lower (0.4 – 2.0 ppm) than at pH 7 as shown in figure 5.14. Following oxygen sparging the dissolved oxygen content showed a progressive increase up to a maximum of 5.7 ppm for the collectorless test, 6.6 ppm for the SNPX test, 7.7 ppm for the SIBX with copper test and up to 8.6 ppm for the SIBX test. Once the maximum dissolved oxygen content had been reached, the decay of dissolved oxygen with time was fastest for the collectorless test (Uptake factor = 60), slightly slower for the xanthate tests (O_2 Uptake factor ~ 24) and slowest for the SIBX with copper test (O_2 Uptake factor = 17).

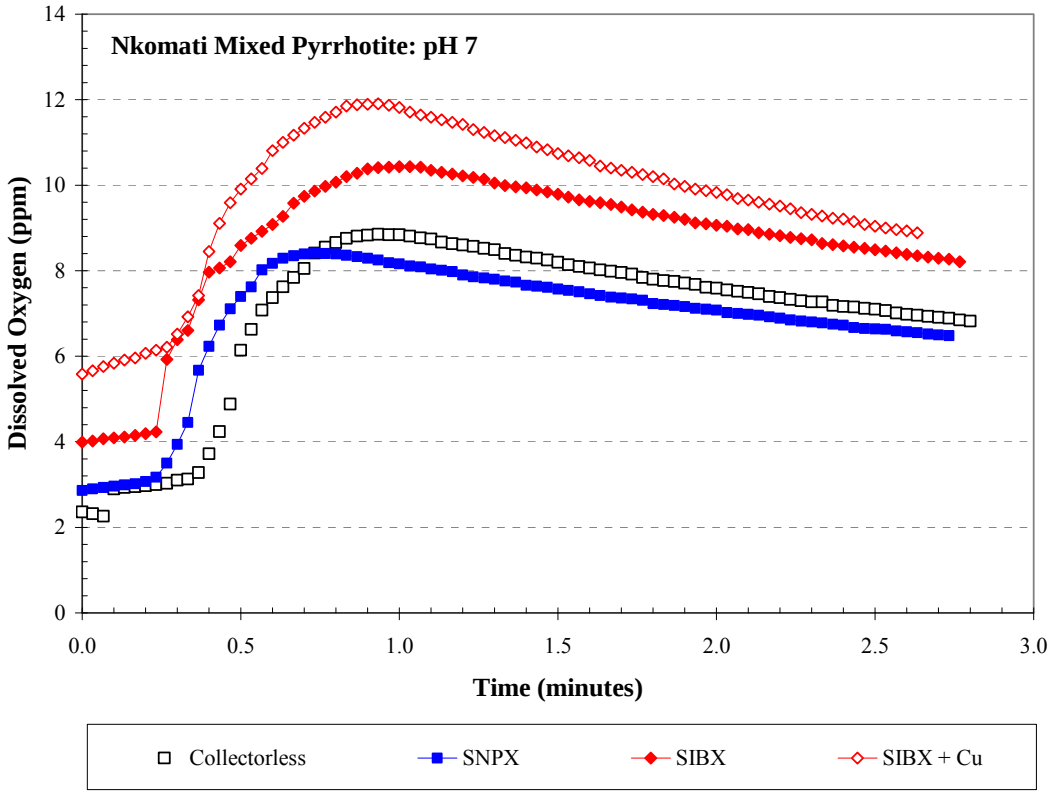

Figure 5.13: Change in dissolved oxygen with time for a slurry containing Nkomati MSB mixed pyrrhotite. Results are shown for the different reagent conditions at pH 7.

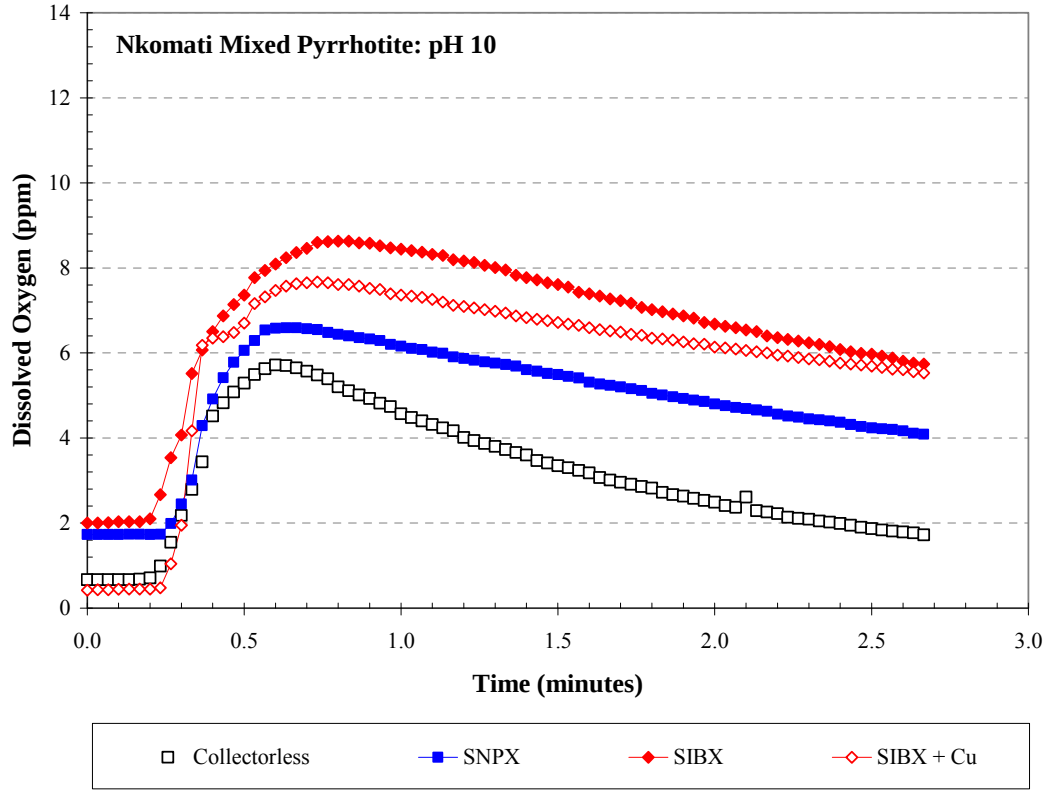

Figure 5.14: Change in dissolved oxygen with time for a slurry containing Nkomati MSB mixed pyrrhotite. Results are shown for the different reagent conditions at pH 10.

5.4.2 Phoenix Pyrrhotite

At pH 7, the natural dissolved oxygen content for a slurry of the Phoenix pyrrhotite prior to oxygen sparging was between 0 and 2 ppm as can be observed in figure 5.15. The natural pH of the slurry was ~ 5, prior to it being altered to the desired pH. Figure 5.15 shows that once the slurry had been sparged with pure oxygen, the dissolved oxygen content showed a steady increase until a point was reached where the rate of oxygen consumption by pyrrhotite oxidation was significant enough to cause a steady decline in the dissolved oxygen content.

At pH 7, the maximum dissolved oxygen content reached for the collectorless test was 6.78 ppm. Slightly higher maximum dissolved oxygen contents were obtained with SIBX (7.64 ppm), and slightly lower maximum dissolved oxygen contents for SNPX (6.88 ppm). With SIBX and copper addition, even higher maximum dissolved oxygen contents were obtained, whereas for SNPX with copper addition the lowest dissolved oxygen contents were measured at this pH.

The natural dissolved oxygen contents for Phoenix magnetic pyrrhotite at pH 10 are shown in figure 5.16 where it is evident that they were all less than 1 ppm and as such, even lower than at pH 7. For the collectorless test, the maximum dissolved oxygen content with sparging was the lowest of all (3.91 ppm) and the effect of reagent addition was to increase the maximum dissolved oxygen content. It is also apparent that at pH 10, the effect of copper addition with xanthate was to cause higher maximum dissolved oxygen contents (e.g. 6.25 ppm for SIBX and 7.16 ppm for SIBX + Cu).

The calculated oxygen uptake factors for the Phoenix magnetic pyrrhotite reactivity tests given in table 5.2 were as high as 29 at pH 7 and for pH 10, as high as 110. For both the pH conditions tested, the highest oxygen uptake factors were obtained for the collectorless tests (O_2 uptake factor = 29 at pH 7, 110 at pH 10). The effect of reagent addition was to decrease the oxygen uptake factor e.g. decrease to 24 at pH 7 for SNPX. A further decrease in oxygen uptake factor was observed with the addition of copper e.g. decrease to 16 at pH 7 for SNPX + Cu. The effect of an increase in pH was to cause a further increase in oxygen uptake factor, e.g. increase up to 60 for SNPX at pH 10. Similarly, the effect of copper addition at pH 10 was to cause another decrease in oxygen uptake factor, e.g. decrease to 28 for SNPX + Cu.

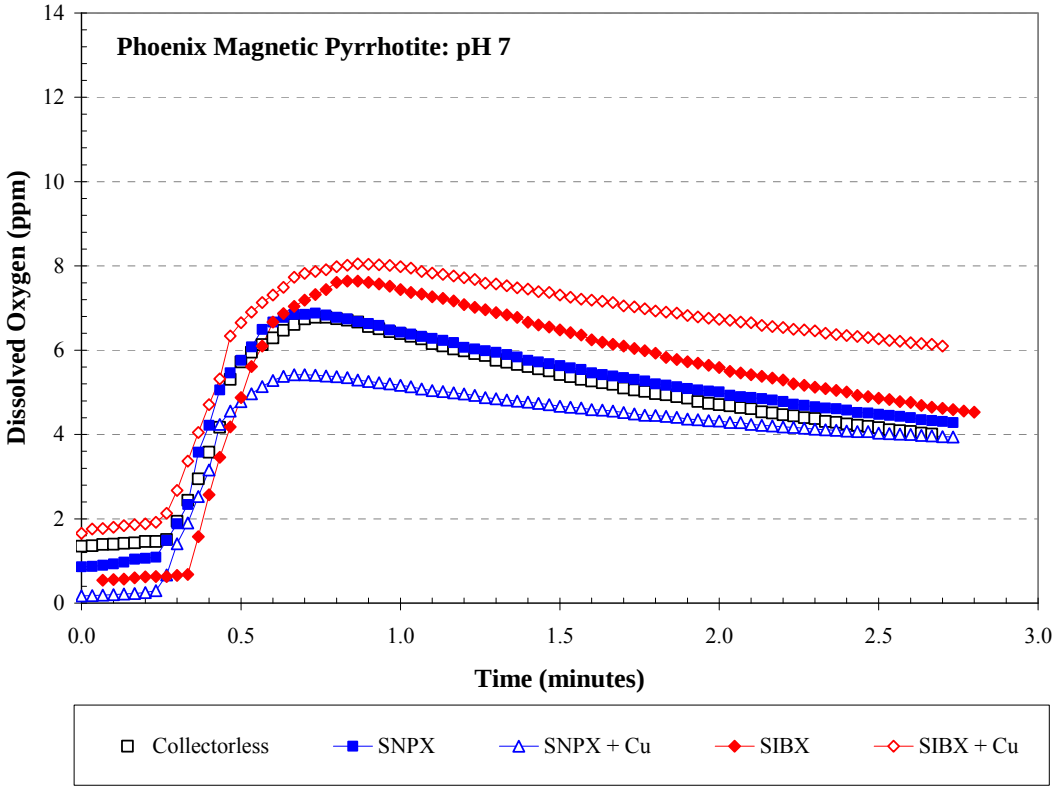

Figure 5.15: Change in dissolved oxygen with time for a slurry containing magnetic Phoenix pyrrhotite. Results are shown for the different reagent conditions at pH 7.

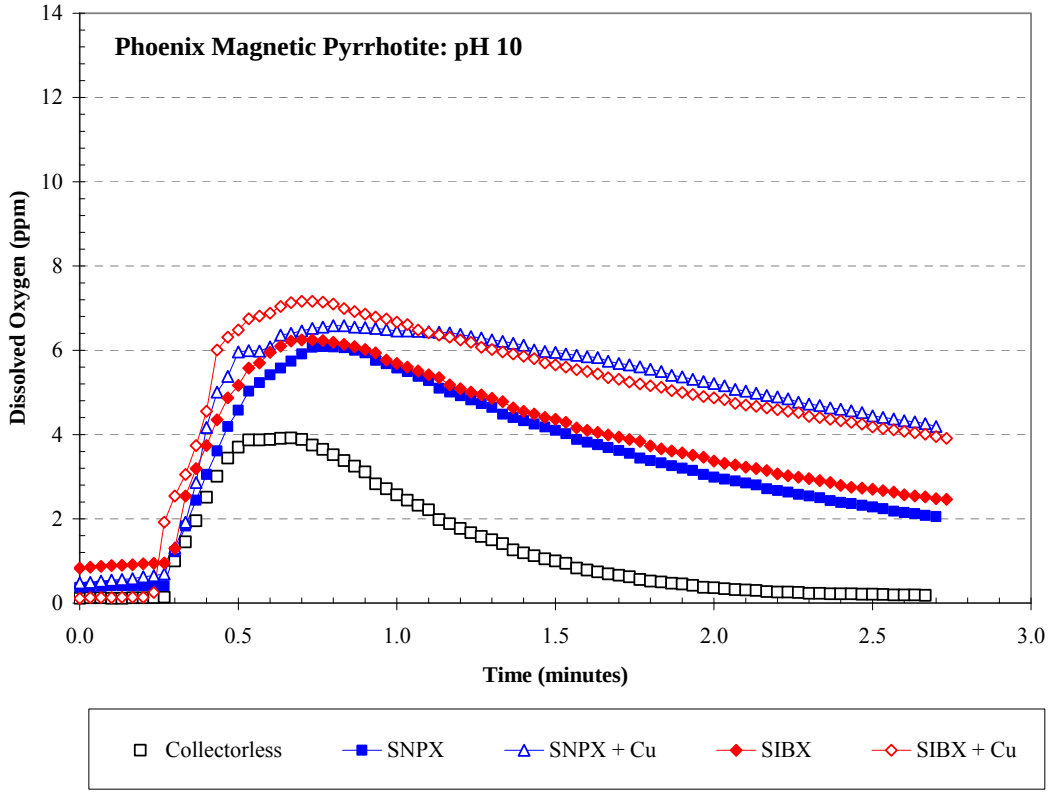

Figure 5.16: Change in dissolved oxygen with time for a slurry containing magnetic Phoenix pyrrhotite. Results are shown for the different reagent conditions at pH 10.

5.4.3 Sudbury Copper Cliff North Pyrrhotite

Following reagent conditioning, the natural pH measured for the Sudbury CCN non-magnetic pyrrhotite slurry was ~ 8 prior to pH modification associated with the mineral reactivity tests. The natural dissolved oxygen content at both pH 7 and 10 varied between 6 and 7.5 ppm as can be observed in figures 5.17 and 5.18. With oxygen sparging, the dissolved oxygen in the Sudbury CCN pyrrhotite slurry showed a rapid increase followed by a sudden, yet slow decay in dissolved oxygen due to the oxidation of the pyrrhotite in the slurry. The highest maximum dissolved oxygen content was obtained for the SIBX with copper test at pH 7 (13.3 ppm). For all the tests at pH 7, the consequent drop in dissolved oxygen content with time following oxygen sparging tended to be slow and therefore the calculated oxygen uptake factors were low (≤ 12; Table 5.1). Given the low oxygen uptake factors measured, it is unlikely that the differences observed for the different test conditions are significant for the Sudbury CCN non-magnetic pyrrhotite.

For all the tests performed at pH 10, the starting dissolved oxygen content was between 6.6 and 7.4 ppm then showed a sudden increase associated with oxygen sparging as shown in figure 5.18. The subsequent decay in dissolved oxygen due to pyrrhotite oxidation was generally very slow and the dissolved oxygen contents of the slurry remained between approximately 10 and 12 ppm. For the SIBX tests, the addition of copper caused an increase in maximum dissolved oxygen content (11.5 ppm for SIBX, 12.7 ppm for SIBX + Cu), and similarly for SNPX at pH 10. In terms of the calculated oxygen uptake factors, the addition of collector caused a decrease in uptake factor (O_2 uptake factor = 6 for both SNPX and SIBX) relative to the blank test (O_2 Uptake factor = 8). The addition of copper however had varying effects; an associated increase in oxygen uptake factor was observed for SIBX with copper addition (10) whereas for SNPX with copper addition, a decrease was observed (2). Similarly to at pH 7, the disparity in the calculated oxygen uptake factors for the CCN pyrrhotite is most likely a consequence of the error associated with the actual measurement.

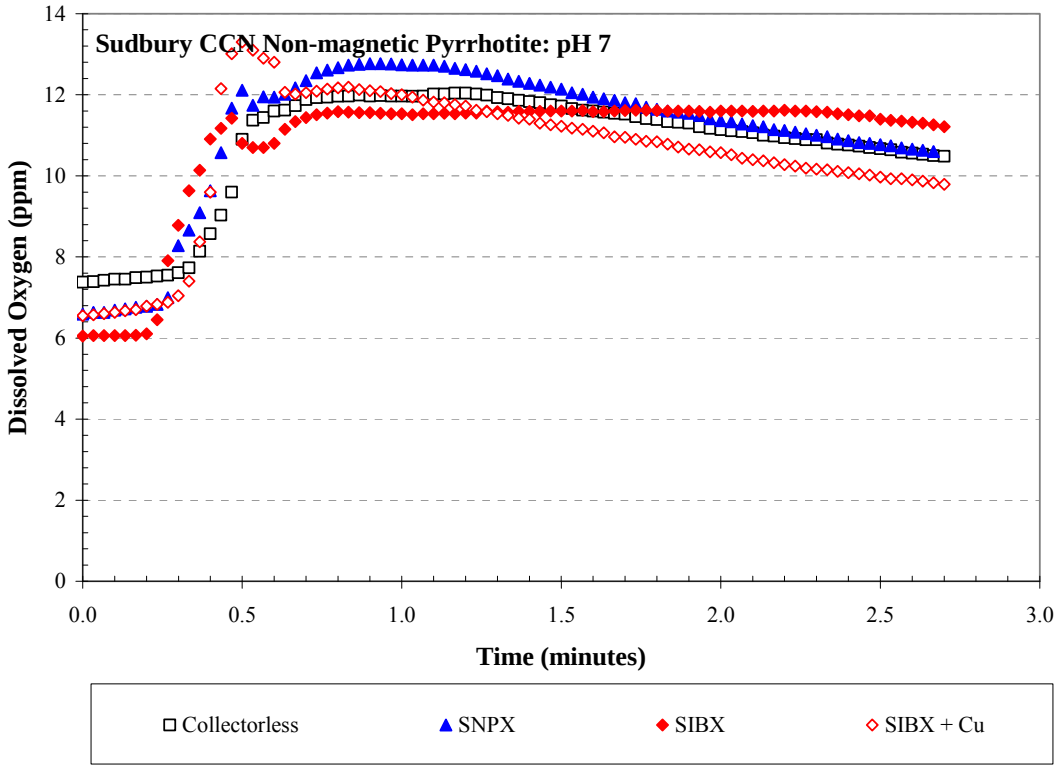

Figure 5.17: Change in dissolved oxygen with time for a slurry containing non-magnetic Sudbury CCN pyrrhotite. Results are shown for the different reagent conditions at pH 7.

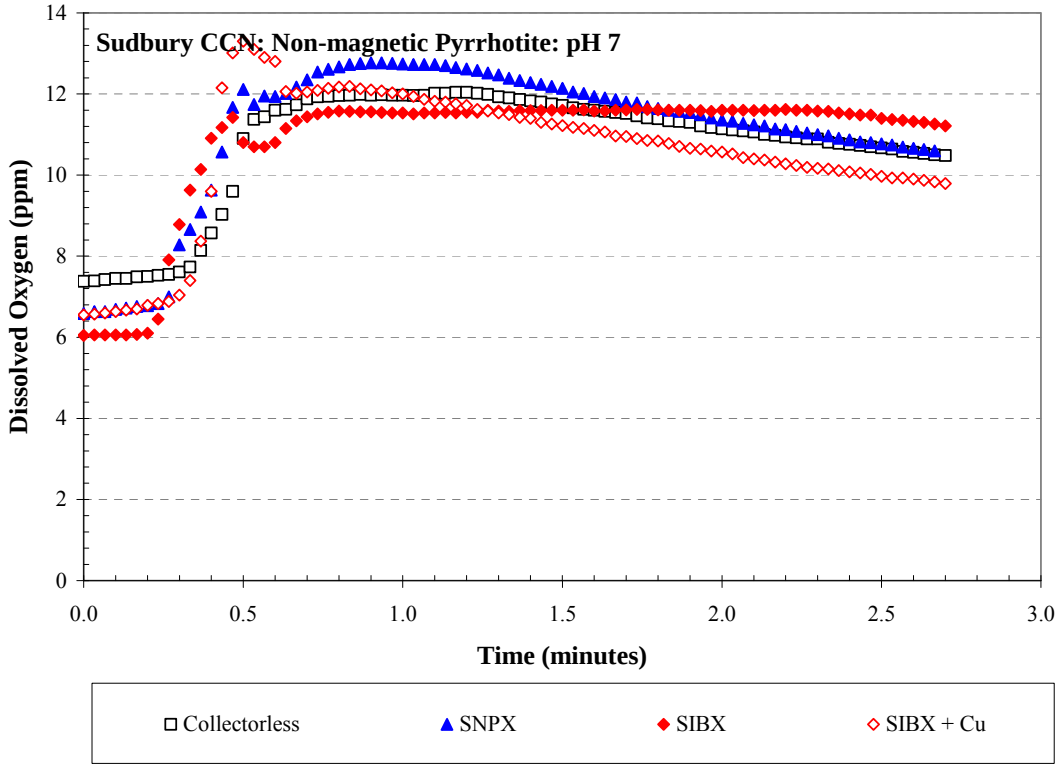

Figure 5.18: Change in dissolved oxygen with time for a slurry containing non-magnetic Sudbury CCN pyrrhotite. Results are shown for the different reagent conditions at pH 10.

5.4.4 Sudbury Gertrude West Pyrrhotite

Magnetic Sudbury Gertrude West pyrrhotite had a neutral pH (~ 7) when made into a mineral slurry prior to pH modification for the associated mineral reactivity tests. Prior to oxygen sparging the dissolved oxygen content of the mineral slurry varied between 1.8 and 3.6 ppm as shown in figure 5.19. Following sparging with oxygen, the dissolved oxygen content of the pyrrhotite slurry climbed to above 7.5 ppm, before the oxidation of pyrrhotite started to consume the dissolved oxygen in solution. At this point, the measured dissolved oxygen content of the slurry decreased at a relatively slow rate. For all tests other than the SNPX with copper test, slightly lower maximum dissolved oxygen contents were measured relative to the collectorless test.

In terms of the rate of dissolved oxygen consumption as quantified by the calculated oxygen uptake factor given in table 5.1, the highest factor was obtained for the collectorless test (O_2 Uptake factor = 17) and lower factors were obtained for tests with reagent addition. For both the SNPX and SIBX tests, the addition of copper caused an associated decrease in pyrrhotite reactivity (i.e. slower rate of O_2 decay) and lower oxygen uptake factors were obtained (e.g. O_2 Uptake factor = 12 for SIBX, 9 for SIBX + Cu).

It is noted that the slurry containing Gertrude West magnetic pyrrhotite was more reactive at pH 10 relative to pH 7 as shown in figure 5.20. The maximum dissolved oxygen contents measured for all the test conditions were lower at pH 10 (< 8.2 ppm) than at pH 7 (up to 9.8 ppm). It is also apparent that the slopes of the graphs in figure 5.20 were steeper for the tests at pH 10 than at pH 7 and which were manifested by the difference in calculated oxygen uptake factors for the Gertrude West pyrrhotite. In general, the calculated oxygen uptake factors at pH 10 were approximately double that from at pH 7, e.g. O_2 Uptake factor = 17 at pH 7, 36 at pH 10 for collectorless test. Calculated oxygen uptake factors were also lower with the addition of SIBX (29) or SNPX (33), and even lower still, with the addition of copper (O_2 Uptake factor = 13 for SIBX + Cu, 14 for SNPX + Cu).

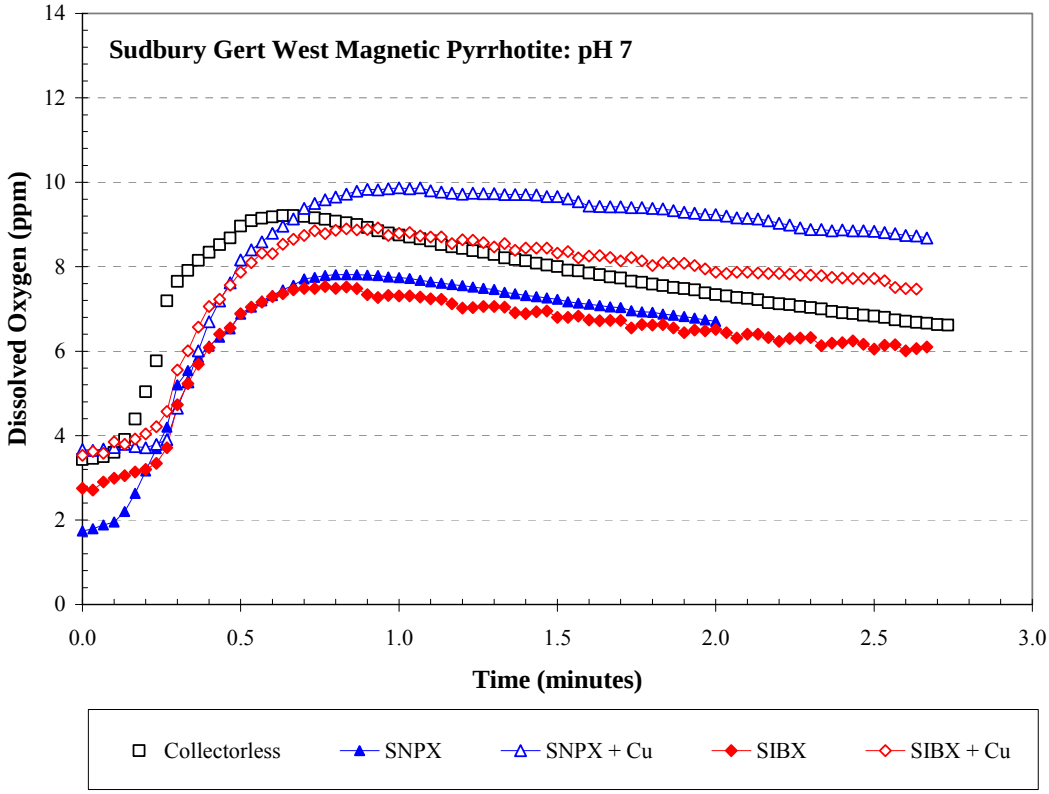

Figure 5.19: Change in dissolved oxygen with time for a slurry containing magnetic Sudbury Gertrude West pyrrhotite. Results are shown for the different reagent conditions at pH 7.

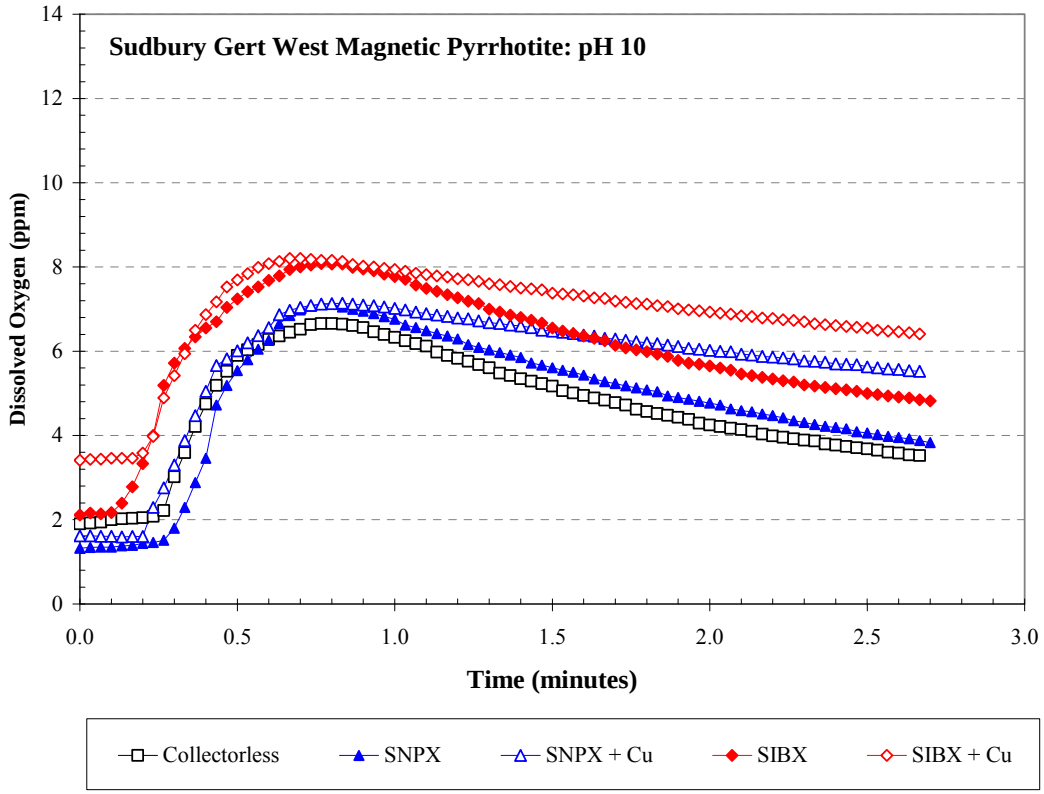

Figure 5.20: Change in dissolved oxygen with time for a slurry containing magnetic Sudbury Gertrude West pyrrhotite. Results are shown for the different reagent conditions at pH 10.

5.4.5 Comparison of the Oxygen Uptake of Pyrrhotite Samples

A comparison of the change in dissolved oxygen content with time for the four pyrrhotite slurries investigated is shown for pH 7 and pH 10 in figures 5.21 and 5.22, respectively. For comparative purposes, the results from only the collectorless tests are shown so that the interpretation is not complicated by the interaction of the reagents with the pyrrhotite surface. Figure 5.21 shows that at pH 7, the natural dissolved oxygen content was quite different for the slurries of the four pyrrhotite samples. The natural dissolved oxygen content of Phoenix magnetic pyrrhotite was lowest, the Nkomati mixed pyrrhotite was slightly higher, the magnetic Sudbury Gertrude West pyrrhotite was even higher, and the Sudbury CCN non-magnetic pyrrhotite was by far the highest of all. Following sparging with oxygen, the maximum dissolved oxygen contents of the pyrrhotite slurries showed a similar ordering; Phoenix magnetic pyrrhotite was the lowest (6.8 ppm), the Nkomati mixed pyrrhotite was slightly higher (8.8 ppm), the magnetic Sudbury Gertrude West pyrrhotite was even higher (9.2 ppm) and the Sudbury CCN non-magnetic pyrrhotite was by far the highest (12.0 ppm). This order was in turn reversed when the oxygen uptake factors are compared, in that the pyrrhotite with the highest dissolved oxygen contents (Sudbury CCN) had the lowest oxygen uptake factor (9), those with intermediate dissolved oxygen contents (Nkomati, Sudbury Gertrude West) had moderate oxygen uptake factors (~15), and the pyrrhotite with the lowest dissolved oxygen content (Phoenix) had the highest oxygen uptake factor (29).

Figure 5.22 shows that the relative differences in mineral reactivity between slurries of the four pyrrhotite samples at pH 7 were conserved at pH 10, although the differences were more extreme. For the magnetic and mixed pyrrhotite samples, the natural dissolved oxygen content was distinctly lower at pH 10 (< 2 ppm) and even approached zero for the Phoenix magnetic pyrrhotite. The natural dissolved oxygen content of the non-magnetic Sudbury CCN appeared to be relatively unaffected by a change in pH. In terms of the uptake of dissolved oxygen in solution through pyrrhotite oxidation, magnetic Phoenix pyrrhotite was the greatest (O_2 Uptake factor = 110), mixed Nkomati pyrrhotite was slightly less (O_2 uptake factor = 60), magnetic Sudbury Gertrude West was even less (O_2 uptake factor = 36) and the non-magnetic Sudbury CCN pyrrhotite was the lowest (O_2 uptake factor = 8). This indicates that the non-magnetic Sudbury CCN pyrrhotite was the least reactive of the pyrrhotite samples examined and had the lowest propensity for oxygen consumption via pyrrhotite oxidation.

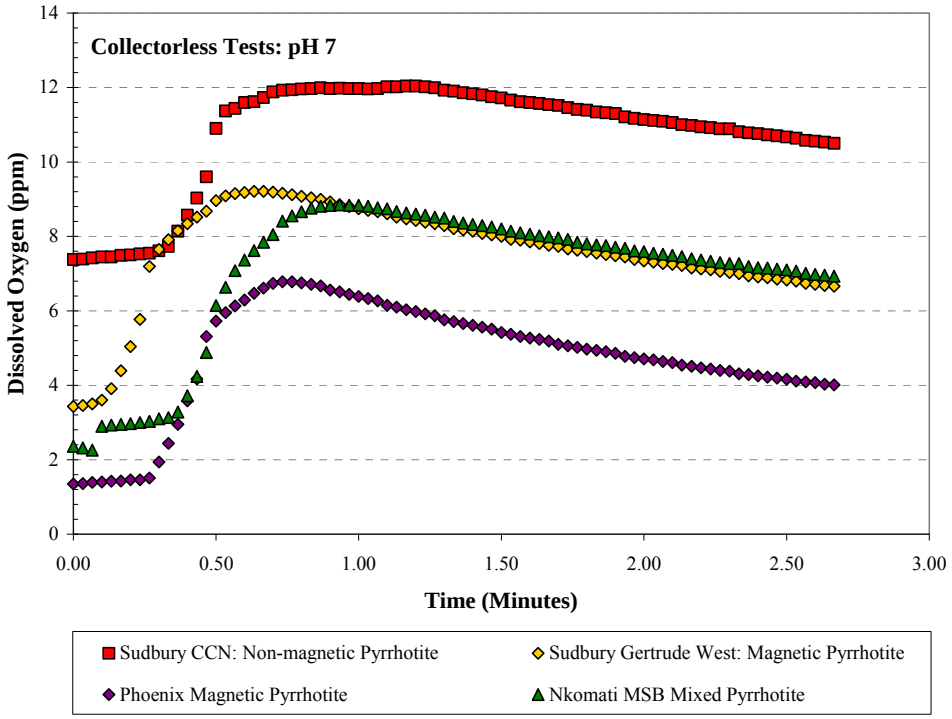

Figure 5.21: Change in dissolved oxygen content with time for slurries of all the pyrrhotite samples at pH 7 shown for the collectorless tests.

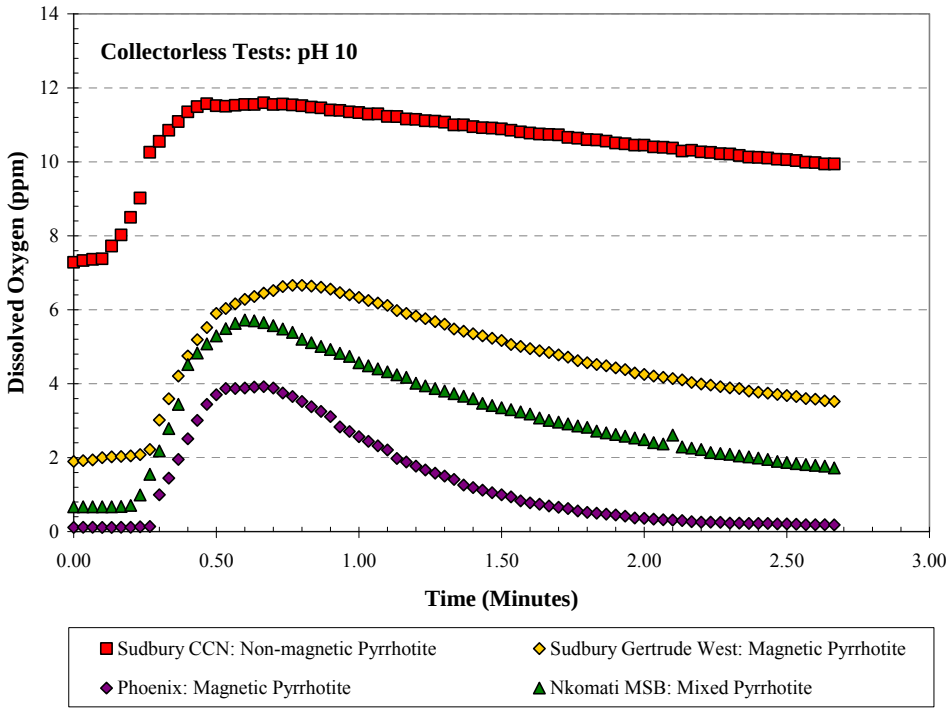

Figure 5.22: Change in dissolved oxygen content with time for slurries of all the pyrrhotite samples at pH 10 shown for the collectorless tests.

Comparison of the oxygen uptake factors at pH 7 for slurries of the four pyrrhotite samples examined under various reagent conditions illustrated in figures 5.23 and 5.24 shows that the Phoenix magnetic pyrrhotite always had the highest oxygen uptake factor for the conditions investigated. Similarly, the calculated oxygen uptake factors were almost always the lowest for the non-magnetic Sudbury CCN pyrrhotite, whereas the calculated oxygen uptake factors were generally slightly lower and similar for the magnetic Gertrude West and mixed Nkomati pyrrhotite samples.

The general trend observed at pH 7 with respect to the effect of reagent addition on the calculated oxygen uptake factor was that the factor got smaller since the addition of collector retarded the decay of oxygen in the pyrrhotite slurry (Figure 5.23, 5.24). Similarly, even though the trend appears to be somewhat tentative, the addition of copper to the solution caused a further drop in the oxygen uptake factor, suggesting the decay of oxygen in the pyrrhotite slurry was retarded even more.

Comparison of the calculated oxygen uptake factors in the collectorless oxygen uptake tests of the four pyrrhotite slurries at pH 10 illustrated in figures 5.25 and 5.26 similarly shows that the Phoenix magnetic pyrrhotite always had the highest oxygen uptake factor. In contrast, the oxygen uptake factors were always the lowest for the non-magnetic Sudbury CCN pyrrhotite slurry whereas oxygen uptake factors were somewhere in between for the magnetic Sudbury Gertrude and mixed Nkomati pyrrhotite samples. In general, the effect of collector addition on the reactivity for oxygen consumption of all the pyrrhotite slurries at pH 10 was to reduce their reactivity as shown by the decrease in calculated oxygen uptake factors. In general, the reactivity of the pyrrhotite with SNPX addition was greater than with SIBX addition. The effect of copper addition in conjunction with SIBX or SNPX addition was to cause a further decrease in pyrrhotite reactivity as evidenced by the subsequent decrease in oxygen uptake figures. It is evident however, that the oxygen uptake factors for the non-magnetic Sudbury CCN pyrrhotite showed little change that could be correlated with the effect of reagent addition which is an indication of the relatively unreactive nature of this pyrrhotite sample.

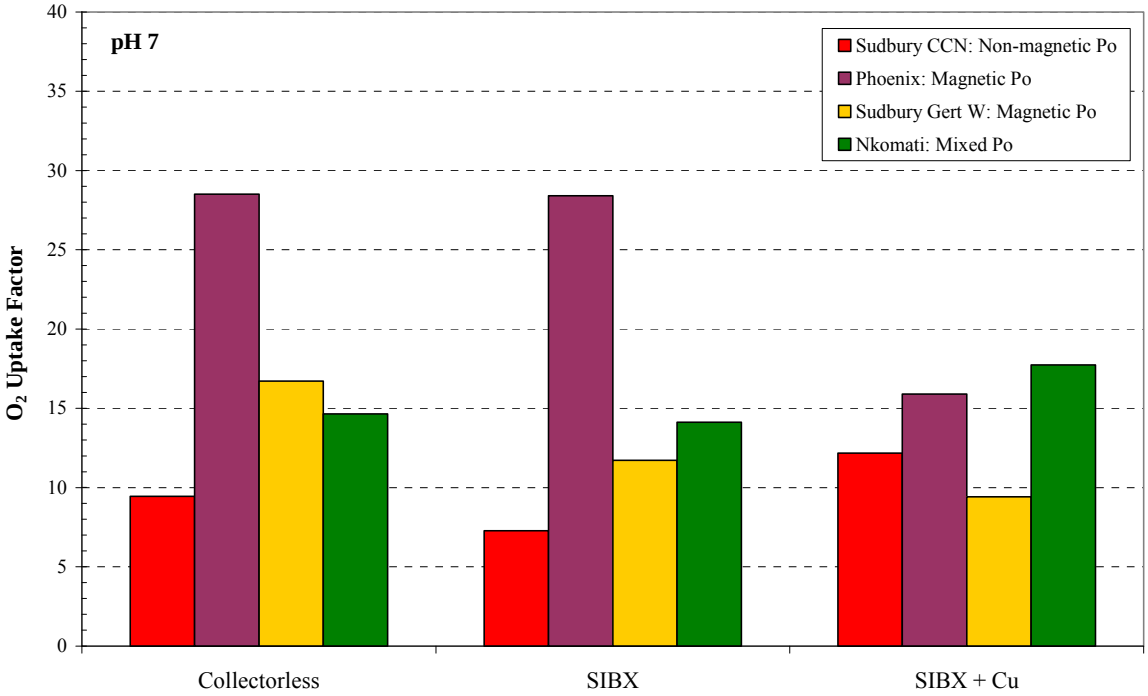

Figure 5.23: Comparison of the dissolved oxygen uptake factor for slurries of all the pyrrhotite samples at pH 7 shown for SIBX collector tests.

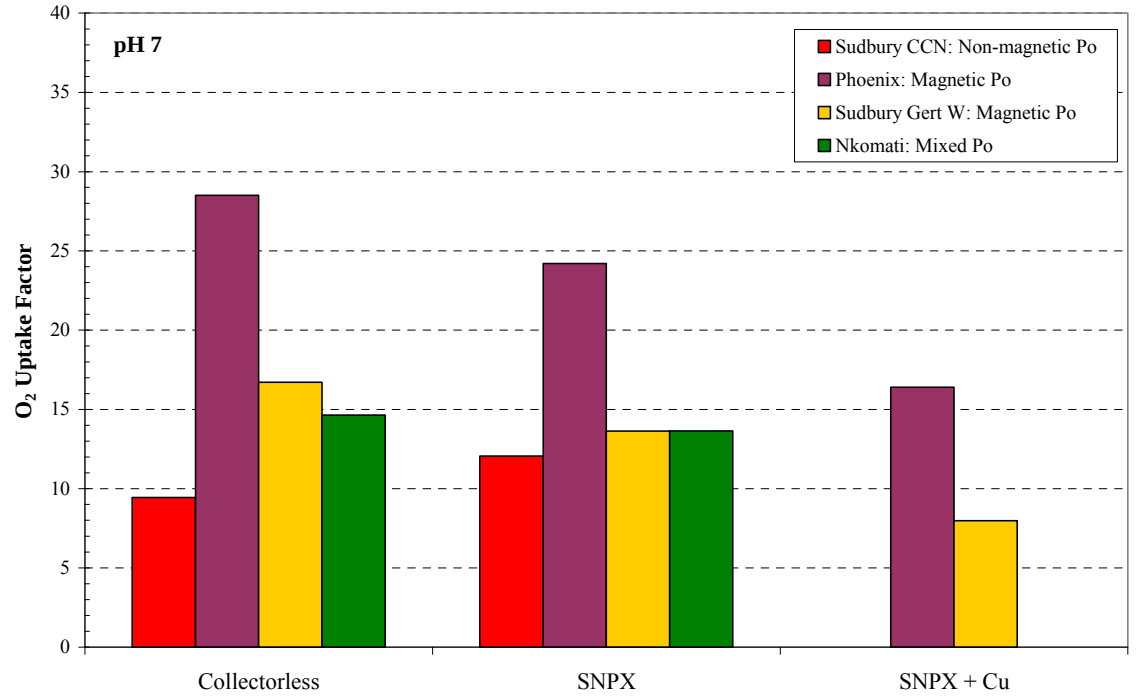

Figure 5.24: Comparison of the dissolved oxygen uptake factor for slurries of all the pyrrhotite samples at pH 7 shown for SNPX collector tests.

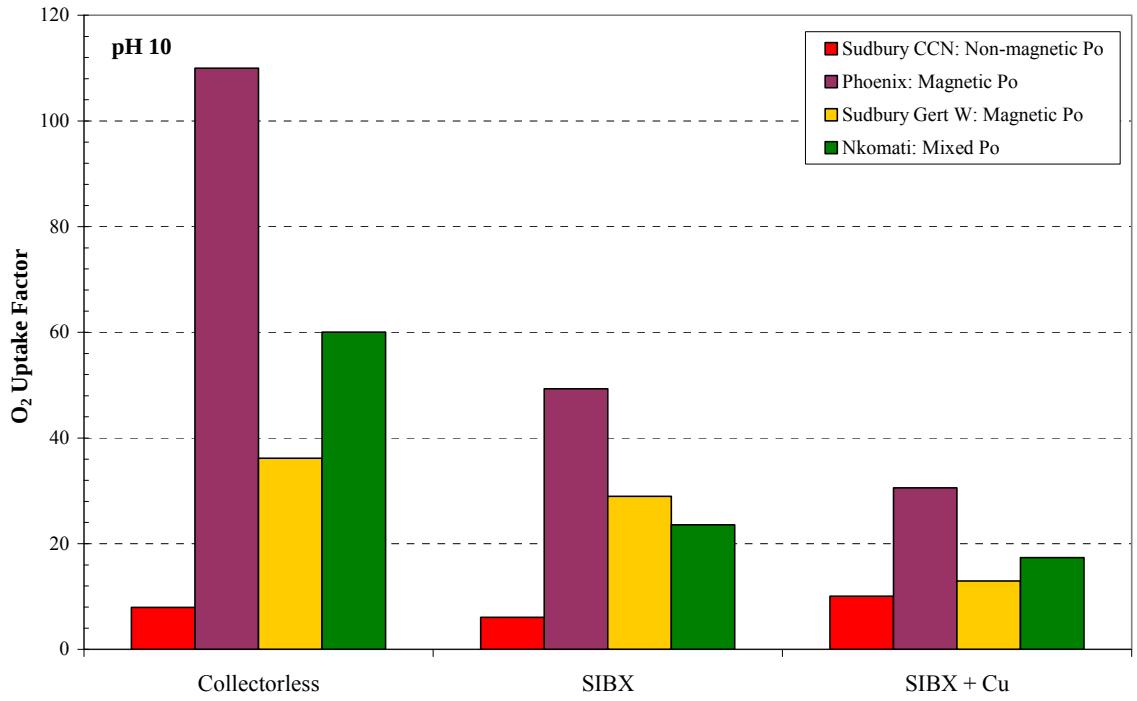

Figure 5.25: Comparison of the dissolved oxygen uptake factor for slurries of all pyrrhotite samples at pH 10 shown for SIBX collector tests.

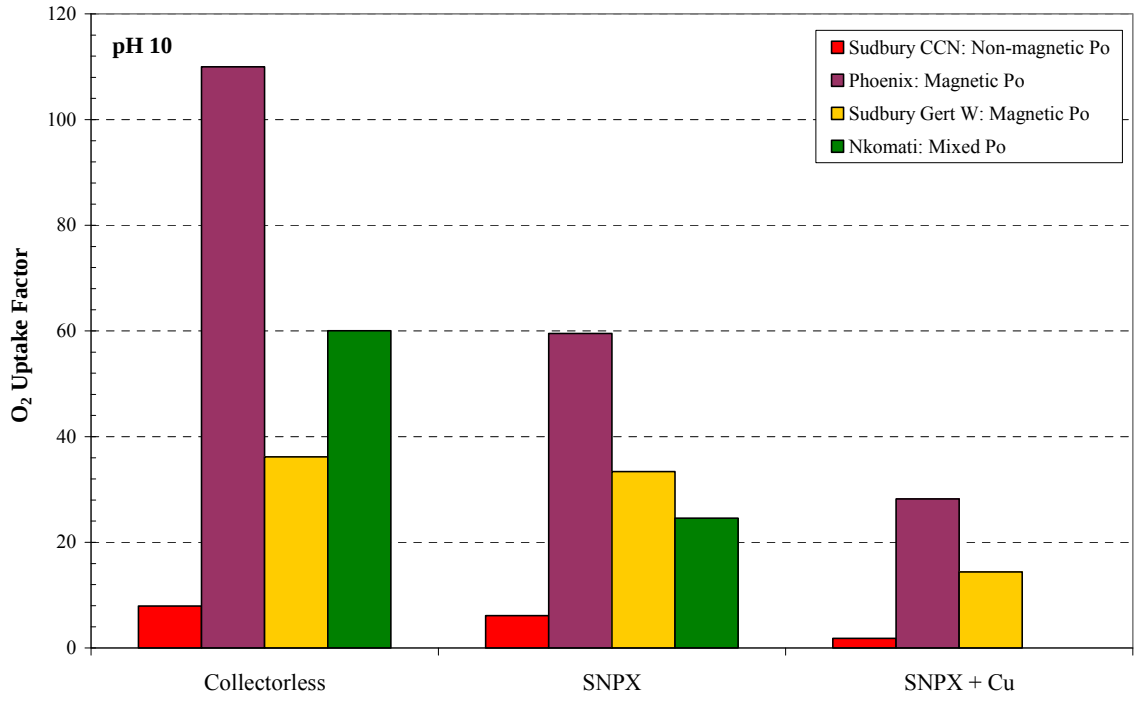

Figure 5.26: Comparison of the dissolved oxygen uptake factor for slurries of all pyrrhotite samples at pH 10 shown for SNPX collector tests.

5.5 Key findings

Key features noted with respect to the reactivity of pyrrhotite from selected nickel and platinum group element ore deposits were as follows:

Open circuit potential measurements performed on electrodes of the four pyrrhotite samples at pH 7 were relatively similar to each other, although the Sudbury CCN non-magnetic pyrrhotite was observed to show the highest open circuit potential (170 mV). At pH 10, better resolution occurred between open circuit potential measurements of the different pyrrhotite electrodes due to differences in electrochemical reaction rates. The highest open circuit potential was obtained for the Sudbury Gertrude West magnetic pyrrhotite sample (116 mV) and which indicated that the pyrrhotite electrode was the most oxidised of the samples examined. Phoenix magnetic pyrrhotite and Nkomati MSB mixed pyrrhotite had slightly lower and similar open circuit potentials (~ 43mV), and the lowest open circuit potential was obtained for the Sudbury CCN non-magnetic pyrrhotite (15 mV).

Two anodic and three cathodic reactions were noted in the cyclic voltammetry studies of the four pyrrhotite electrodes at pH 7. At pH 10, three anodic and two cathodic reactions were noted in the cyclic voltammetry studies. These reactions were common to all four pyrrhotite samples except for the Sudbury CCN non-magnetic pyrrhotite that did not show the anodic reaction A3 at ~ -200mV at pH 10. Significant differences were observed in current density that were related to differences in electrochemical reaction rates and pyrrhotite reactivity. Sudbury CCN non-magnetic pyrrhotite showed the smallest change in current density, Nkomati MSB mixed pyrrhotite showed slightly greater changes in current density and Phoenix magnetic pyrrhotite showed even greater changes in current density. The Gertrude West magnetic pyrrhotite showed the greatest changes in current density and was therefore the most reactive of the pyrrhotite samples investigated.

The rate of dissolved oxygen uptake from slurries containing the four different pyrrhotite samples increased when the pH was increased from 7 to 10. e.g. The slurry containing Phoenix magnetic pyrrhotite with no collector, showed an increase in the oxygen uptake factor from 29 to 110 due to the increase in reactivity with the increase in hydroxide ion concentration.

The rate of dissolved oxygen uptake from slurries containing the four different pyrrhotite samples decreased with the addition of collector to the slurry e.g. the slurry containing Phoenix magnetic pyrrhotite, showed a decrease in the oxygen uptake factor from 110 to 49 associated with the addition of SIBX at pH 10. The pyrrhotite slurry was noted to be more reactive for the shorter chain length SNPX collector relative to SIBX.

The rate of dissolved oxygen uptake from slurries containing the four different pyrrhotite samples generally decreased with copper activation e.g. the slurry containing Phoenix magnetic pyrrhotite, showed a decrease in the oxygen uptake factor from 49 to 31 associated with copper activation in conjunction with SIBX addition at pH 10.

At both pH 7 and 10, the dissolved oxygen uptake was greatest for the slurry containing the Phoenix magnetic pyrrhotite (O_2 uptake factor = 110 at pH 10). At both pH 7 and 10, the dissolved oxygen uptake was the lowest for the slurry containing the Sudbury CCN non-magnetic pyrrhotite (O_2 uptake factor = 8 at pH 10). The dissolved oxygen uptake was somewhere in between for the Sudbury Gertrude West magnetic and Nkomati MSB mixed pyrrhotite. At pH 10 however, the slurry containing the Nkomati MSB mixed pyrrhotite showed a slightly greater rate of dissolved oxygen uptake (O_2 uptake factor = 60) than the slurry containing Sudbury Gertrude West magnetic pyrrhotite (O_2 uptake factor = 36).

Chapter 6

PYRRHOTITE MICROFLOTATION

6.1 Introduction

As described in Chapter 2, a reasonable understanding exists with regard to the mechanism and species which lend pyrrhotite its floatability but the accounts comparing the floatability of the different pyrrhotite types are in conflict (Section 2.6.3). Since the aim of this research was to develop the relationship between pyrrhotite mineralogy and flotation performance, it is necessary to *explore and compare the flotation performance of magnetic and non-magnetic pyrrhotite*, which is the aim of this chapter. Microflotation tests were selected as the preferred experimental method to compare pyrrhotite flotation since the methodology allows for the flotation of pure sulfide samples. An additional benefit derived from the use of the microflotation, is that no interpretation of the interaction and dynamics between the froth and pulp phases is necessary since there is no froth phase in the microflotation tests (Bradshaw and O'Connor, 1996).

In order to investigate the floatability of pyrrhotite, microflotation tests of the Nkomati MSB mixed pyrrhotite, Phoenix magnetic pyrrhotite, Sudbury CCN non-magnetic pyrrhotite and Sudbury Gertrude and Gertrude West magnetic pyrrhotite samples (Tables 3.1, 3.3) were performed under selected conditions. Flotation tests were conducted with no collector addition (collectorless), collector addition (SIBX or SNPX) and collector plus activator addition (SIBX + Cu, SNPX + Cu). Hydrous copper sulfate ($CuSO_4.5H_20$) was used as a source of copper ions in this study. All tests were conducted with minimal guar depressant (10 ppm) in order to assist with the slime cleaning of pyrrhotite prior to flotation. Due to the very small masses recovered during microflotation tests, chemical assays were not possible for every test condition investigated and therefore the pyrrhotite recovery could not be calculated for every set of tests. Therefore, final mass recovery was chosen as the indicator of pyrrhotite flotation performance for all the samples investigated. It should be noted that the calculated

pyrrhotite recovery in itself was based on the assumption that all the nickel was accounted for by pentlandite recovery, and therefore the calculated pyrrhotite recovery may be slightly underestimated. Additional weaknesses of this assumption are that anomalous pyrrhotite grades are sometimes obtained, given that solid solution nickel was present in varying amounts in the pyrrhotite in this study (Section 4.4), but is the best which was possible within the limitations of this study. Table 6.1 presents a summary of the final mass and calculated pyrrhotite and pentlandite recovery, as well as final pentlandite concentrate grade for the microflotation tests. The complete set of flotation results is presented in Appendix C.

Table 6.1: Summary table of the average final mass, pyrrhotite and pentlandite recovery from microflotation tests of the different pyrrhotite samples. The average final pentlandite grade is also given.

Pyrrhotite Sample	Conditions		Collector-less	SNPX	SNPX+ Cu	SIBX	SIBX + Cu
Nkomati MSB Pyrrhotite Mix	pH 7	Mass Rec (%)	2.87	85.4	80.3	88.1	86.6
		Po Rec (%)	-	90.1	84.9	92.4	90.9
		Pent Rec (%)	-	90.5	85.0	93.8	92.0
		Pent Grade (%)	-	7.00	7.33	7.21	7.39
	pH 10	Mass Rec (%)	2.03	3.85	10.6	5.93	34.5
		Po Rec (%)	-	-	-	-	-
		Pent Rec (%)	-	-	15.2	-	37.3
		Pent Grade (%)	-	-	8.79	-	8.39
Phoenix Magnetic Pyrrhotite	pH 7	Mass Rec (%)	6.15	51.8	70.3	66.3	59.5
		Po Rec (%)	-	51.7	70.4	66.4	59.8
		Pent Rec (%)	14.1	62.9	74.5	73.0	67.0
		Pent Grade (%)	1.36	0.78	0.72	0.74	0.76
	pH 10	Mass Rec (%)	2.71	9.56	42.7	5.54	83.8
		Po Rec (%)	-	-	44.2	-	-
		Pent Rec (%)	5.21	16.0	52.5	14.4	87.6
		Pent Grade (%)	1.43	1.19	0.74	1.72	0.69
Sudbury CCN Non-magnetic Pyrrhotite	pH 7	Mass Rec (%)	36.1	51.6	74.5	68.6	84.6
		Po Rec (%)	-	57.7	85.4	79.1	95.1
		Pent Rec (%)	-	74.6	91.6	89.7	96.4
		Pent Grade (%)	0.61	0.56	0.48	0.49	0.44
	pH 10	Mass Rec (%)	27.0	39.2	54.2	32.7	79.8
		Po Rec (%)	31.2	46.4	60.9	-	91.2
		Pent Rec (%)	42.1	58.1	79.4	47.5	96.4
		Pent Grade (%)	0.61	0.56	0.58	0.71	0.48

Table 6.1: Continued.

Pyrrhotite Sample	Conditions		Collector-less	SNPX	SNPX+ Cu	SIBX	SIBX + Cu
Sudbury Gertrude Magnetic Pyrrhotite	pH 7	Mass Rec (%)	4.79	10.2	17.6	14.7	32.8
		Po Rec (%)	-	-	-	-	-
		Pent Rec (%)	-	-	-	-	-
		Pent Grade (%)	-	-	-	-	-
	pH 10	Mass Rec (%)	5.57	4.44	5.14	5.17	17.4
		Po Rec (%)	-	-	-	-	-
		Pent Rec (%)	-	-	-	-	-
		Pent Grade (%)	-	-	-	-	-
Sudbury Gertrude West Magnetic Pyrrhotite	pH 7	Mass Rec (%)	1.36	14.7	21.9	28.4	41.8
		Po Rec (%)	-	-	-	-	38.8
		Pent Rec (%)	-	33.2	29.4	56.3	58.3
		Pent Grade (%)	-	30.0	18.9	34.7	22.3
	pH 10	Mass Rec (%)	1.36	3.53	4.80	3.77	7.12
		Po Rec (%)	-	-	-	-	-
		Pent Rec (%)	-	-	-	-	-
		Pent Grade (%)	-	-	-	-	-

6.2 Mineralogy of Flotation Feed Samples

Prior to the interpretation of the flotation performance of the various pyrrhotite samples, the mineralogical characteristics of the microflotation feed samples were characterised with a combination of QXRD and MLA techniques (Section 3.2). The more comprehensive MLA results are shown in figures 6.1 to 6.4, so that the role of mineral liberation can be evaluated.

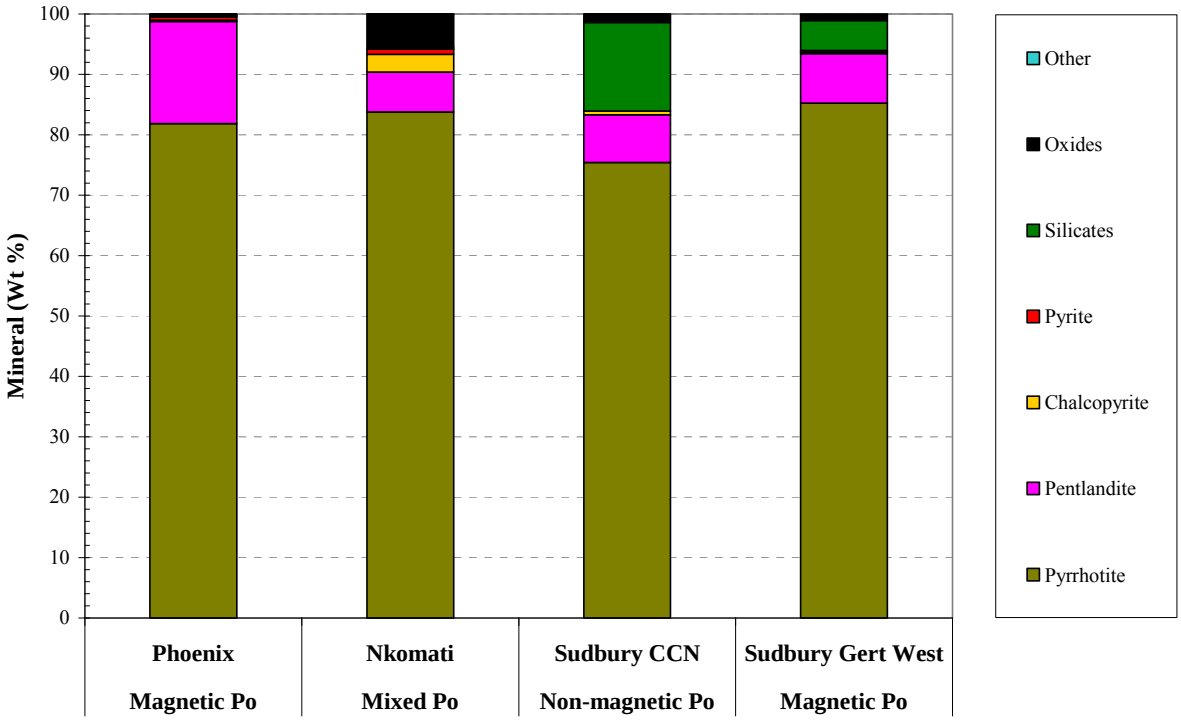

Figure 6.1: Composition of microflotation feed samples for the Nkomati, Sudbury CCN and Sudbury Gertrude West pyrrhotite ores as determined by MLA. The composition of the Phoenix pyrrhotite oxygen uptake sample determined by MLA is also shown and can be assumed to be representative of the Phoenix pyrrhotite microflotation feed sample.

It is evident from figure 6.1 that the pyrrhotite content of all the microflotation feed samples was greater than 75 wt % (see also Table 3.3). The magnetic Sudbury Gertrude West flotation feed sample had the highest pyrrhotite content (85.2 wt %). The concentration of pentlandite in the flotation feed samples varied between 6.61 wt % (Nkomati MSB) and 16.9 wt % (Phoenix). The proportion of chalcopyrite was very low in the flotation feed samples (< 0.66 wt %), except for the Nkomati flotation feed sample which had a chalcopyrite content of 2.29 wt %. Similarly, pyrite content was very low for all the flotation feed samples (< 0.86 wt %).

No pyrite was detected in the Sudbury CCN non-magnetic flotation feed sample. The total base metal sulfide content of the flotation feed samples was the lowest for Sudbury CCN (84.0 wt %), higher for both Sudbury Gertrude West (94.0 wt %) and Nkomati MSB (94.2 wt %), and highest for the Phoenix microflotation feed sample (99.5 wt %). Magnetite was the greatest non-sulfide mineral that contributed to the Nkomati MSB flotation feed sample (5.49 wt %), whereas the silicate minerals (amphibole, biotite, plagioclase and quartz) were the major diluents for both the Sudbury CCN and Gertrude West flotation feed samples (Figure 6.1; Table 3.3).

MLA false colour images of the particle types forming the microflotation feed samples of the various pyrrhotite samples are shown in figure 6.2. Similarly to figure 6.1, these images demonstrate that the microflotation feed samples were dominated by pyrrhotite with some contribution from pentlandite. The Phoenix pyrrhotite sample consisted of pyrrhotite with abundant locked flame pentlandite and only minor liberated granular pentlandite (Figure 6.2a). The Nkomati flotation feed sample also consisted of locked flame pentlandite hosted by pyrrhotite (Figure 6.2b), although considerably less than the Phoenix microflotation feed sample. The Nkomati flotation feed sample also contained some liberated magnetite whereas chalcopyrite occurred in composite particles with pyrrhotite and pentlandite. Pyrrhotite in the Sudbury CCN flotation sample was generally liberated and contained only minor locked flame pentlandite (Figure 6.2c). The pentlandite more commonly occurred as liberated granular pentlandite particles. Silicate gangue minerals in the Sudbury CCN flotation feed sample were generally liberated from the BMS. Similarly to the Sudbury CCN flotation feed sample, Sudbury Gertrude West consisted of liberated pyrrhotite and liberated granular pentlandite (Figure 6.2d). Only minor locked flame pentlandite was apparent. Silicate gangue minerals in the Gertrude West flotation feed sample were also liberated from the BMS.

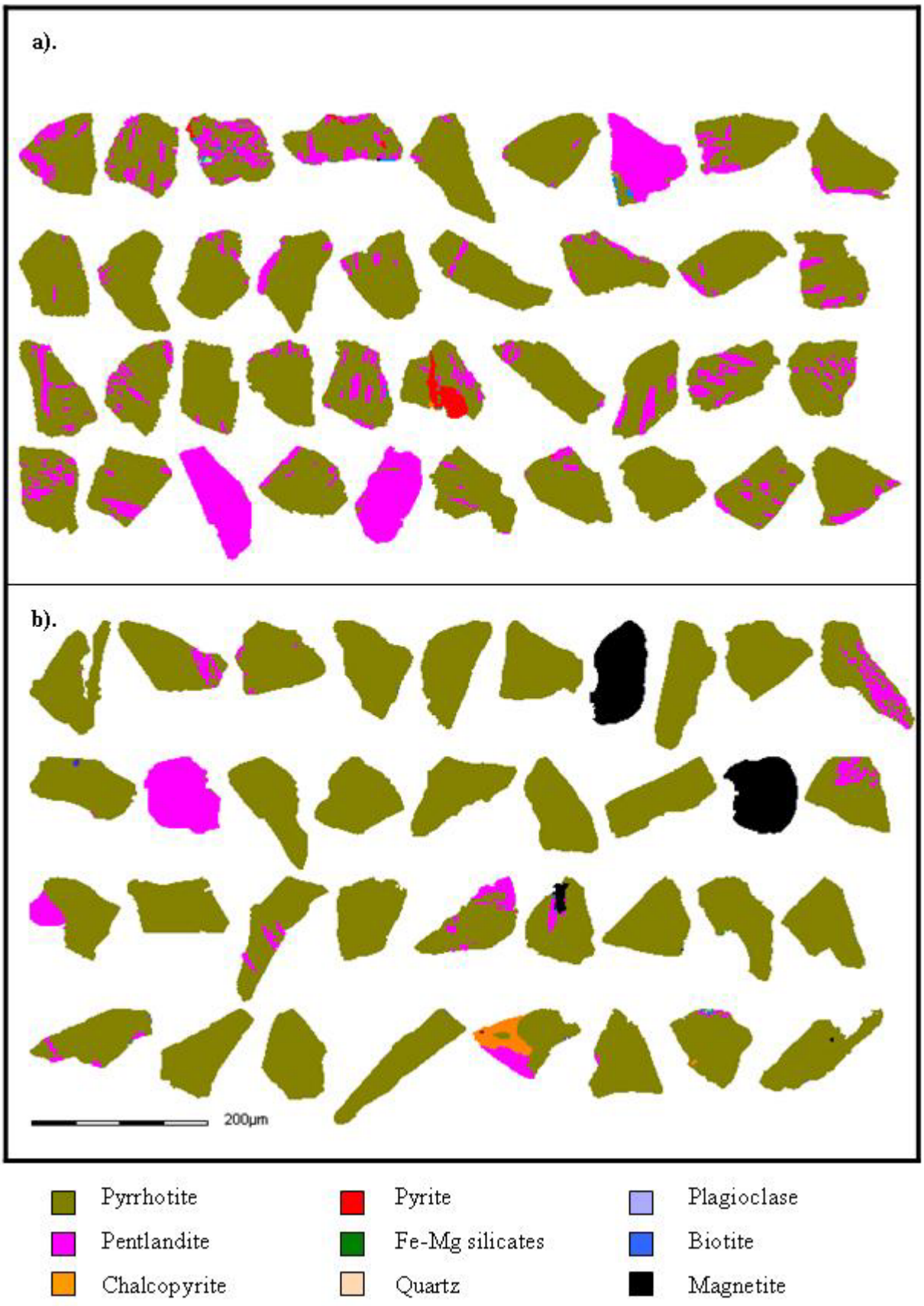

Figure 6.2: MLA particle images of microflotation feed samples shown for (a) Phoenix magnetic pyrrhotite (b) Nkomati mixed pyrrhotite, (c) Sudbury CCN non-magnetic pyrrhotite and (d) Sudbury Gertrude West magnetic pyrrhotite.

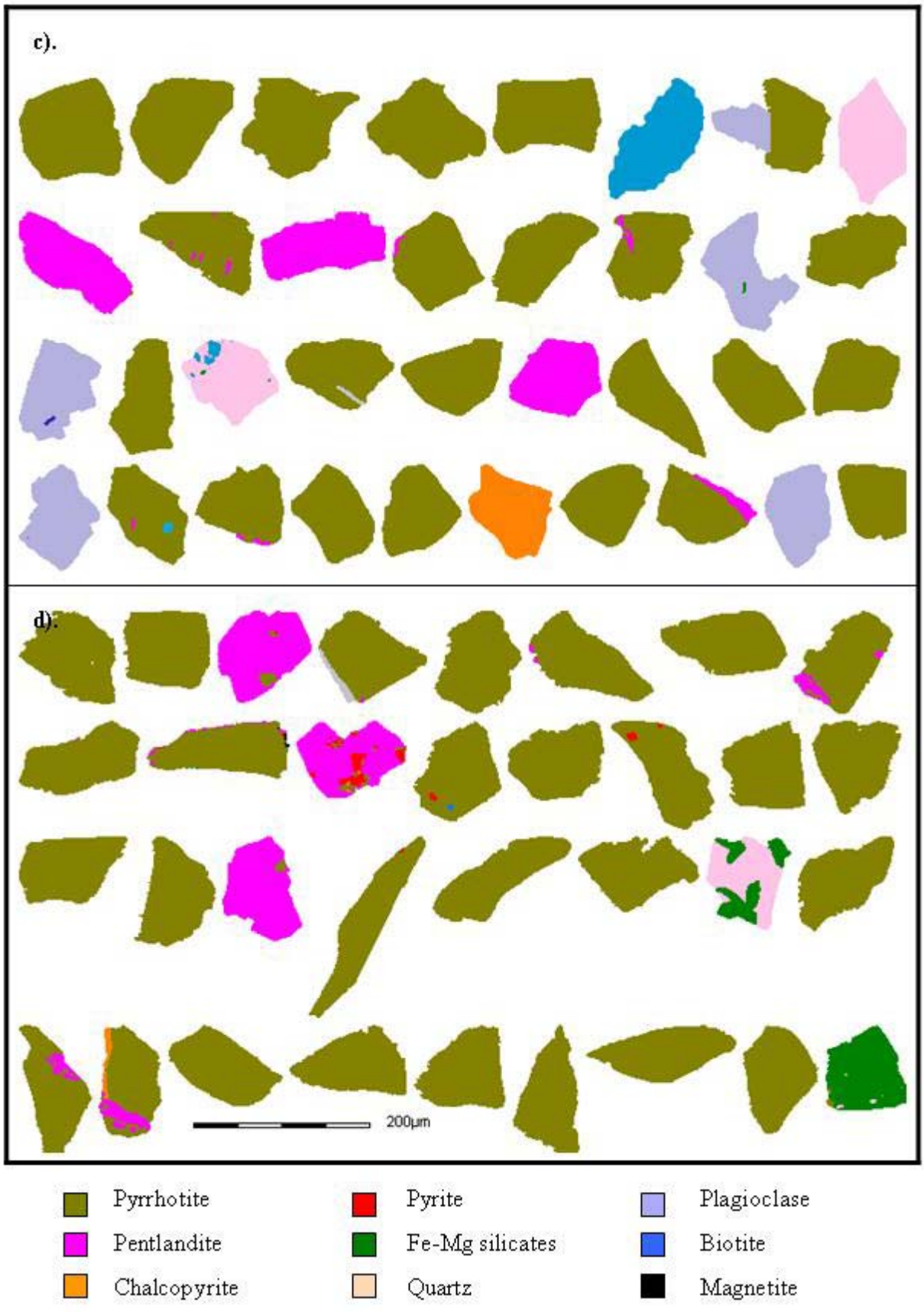

Figure 6.2: Continued.

In order to quantify the observations made from the particle images shown in figure 6.2, the liberation characteristics of pyrrhotite and pentlandite are shown for the microflotation feed samples in figures 6.3 and 6.4, respectively. Pyrrhotite was over 90% liberated (> 95 % area exposed) in the Sudbury CCN and Gertrude West microflotation feed samples (Figure 6.3). Pyrrhotite in the Nkomati microflotation feed sample was only slightly less liberated (88.4 % liberated), whereas Phoenix had considerably lower pyrrhotite liberation (50.7 % liberated). This was due to the significant proportion of locked flame pentlandite in the Phoenix pyrrhotite particles and which is evidenced by the pentlandite liberation characteristics (Figure 6.4). The lowest proportion of liberated pentlandite particles occurred in the Phoenix microflotation feed sample (48.5 % liberated). Pentlandite in the Nkomati microflotation feed sample was only slightly more liberated (53.6 %) due to the fact that less flame pentlandite occurred locked in the pyrrhotite. 77.1 % of the pentlandite particles in the Sudbury Gertrude West microflotation feed were liberated, and 89.3% of the pentlandite particles in the Sudbury CCN microflotation feed sample were liberated (Figure 6.4).

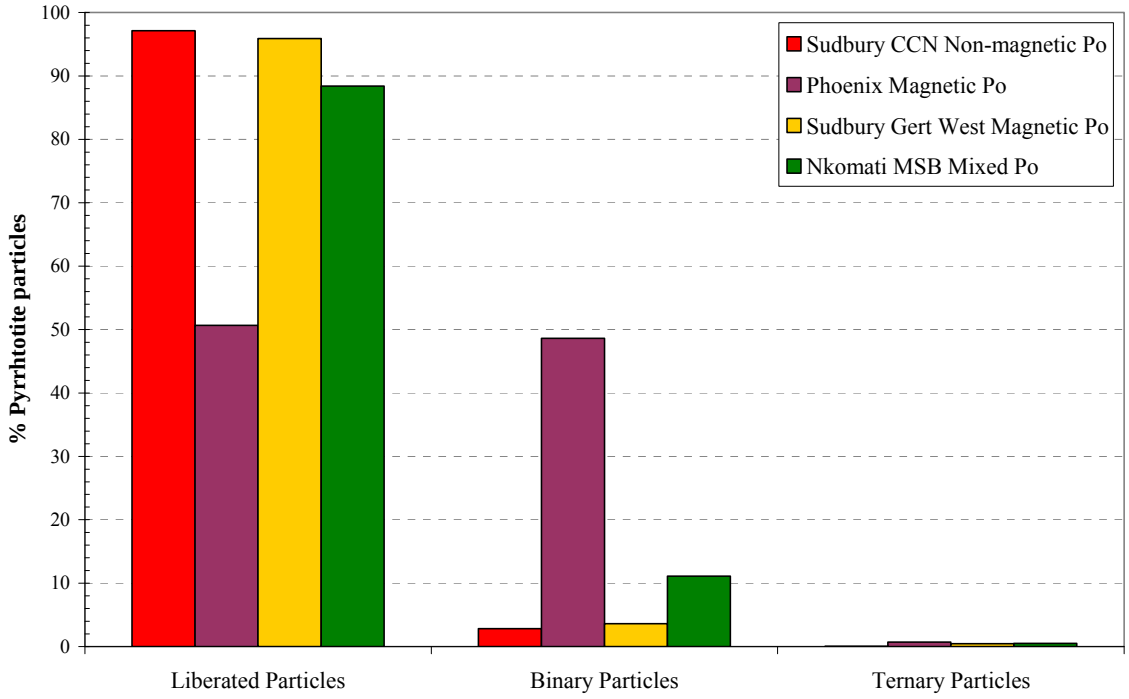

Figure 6.3: Proportion of pyrrhotite in microflotation feed samples as liberated (> 95 % area exposed), binary or ternary particles.

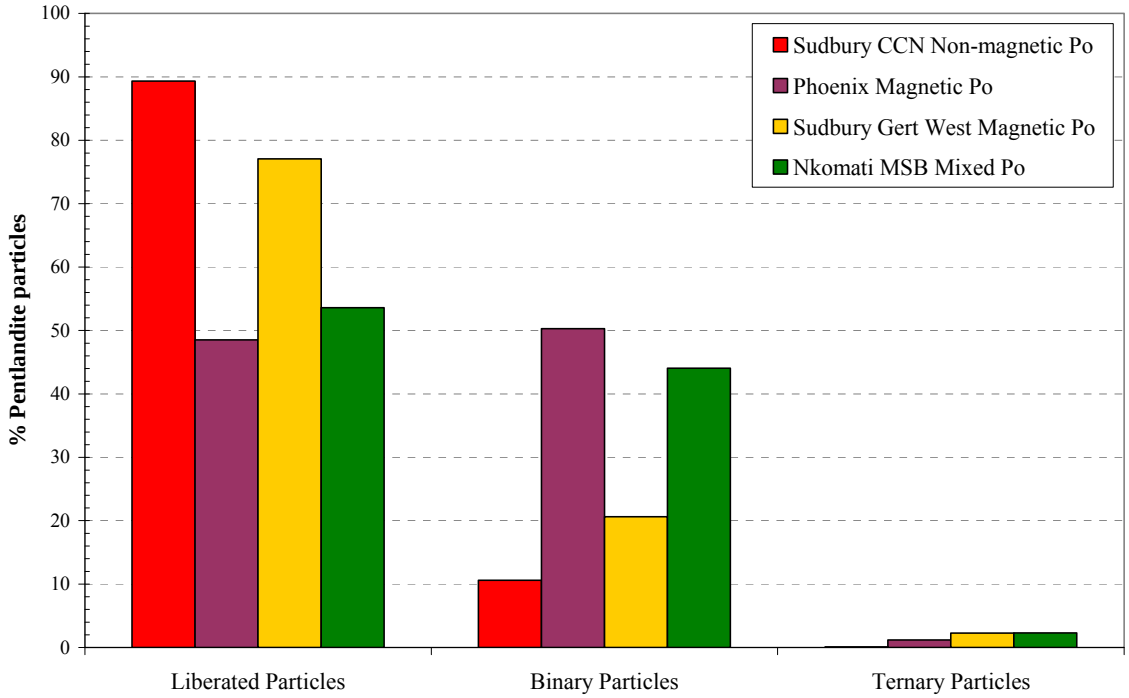

Figure 6.4: Proportion of pentlandite in microflotation feed samples as liberated (> 95% area exposed), binary or ternary particles.

6.3 Nkomati MSB Pyrrhotite

Nkomati MSB mixed pyrrhotite showed poor natural or collectorless floatability at pH 7 as illustrated in figure 6.5, where the mass recovery of the blank flotation test was only 2.87 %. The Nkomati pyrrhotite however, responded very well to the addition of reagents and resulted in a dramatic increase in flotation recovery up to ~ 80 %. Little difference was observed between the conditions of the respective flotation tests with reagent addition. Copper addition appeared to have had no significant impact on the floatability of the Nkomati mixed pyrrhotite at pH 7. For the SNPX flotation test with copper activation, a slightly lower overall recovery of pyrrhotite was obtained during flotation (decrease from 85.4 to 80.3 % recovery).

Similarly to the microflotation results at pH 7, the natural floatability of Nkomati pyrrhotite at pH 10 shown in figure 6.6 was very poor (2.03 % recovery). The addition of xanthate collector caused a subtle improvement in overall pyrrhotite floatability up to ~ 5 % mass recovery. Nkomati pyrrhotite floatability was further improved by the addition of copper in conjunction with SNPX (10.6 % recovery). The effect of copper activation in conjunction with the stronger SIBX collector caused a further increase in mass recovery up to 34.5 %, but this was still well below the flotation recovery obtained at pH 7.

Compared to the actual mass recovery, the calculated pyrrhotite recovery for Nkomati pyrrhotite for the various flotation tests given in table 6.1 was ~ 5 % higher than the mass recovery. Similarly, pentlandite recovery was also ~ 5 % higher than the mass recovery. The grade of pentlandite in the concentrates collected in the microflotation test was between 7 and 8 wt %. Therefore, it needs to be considered that the good flotation performance of the Nkomati pyrrhotite induced by reagent addition was somewhat influenced by the recovery of pentlandite to the concentrate.

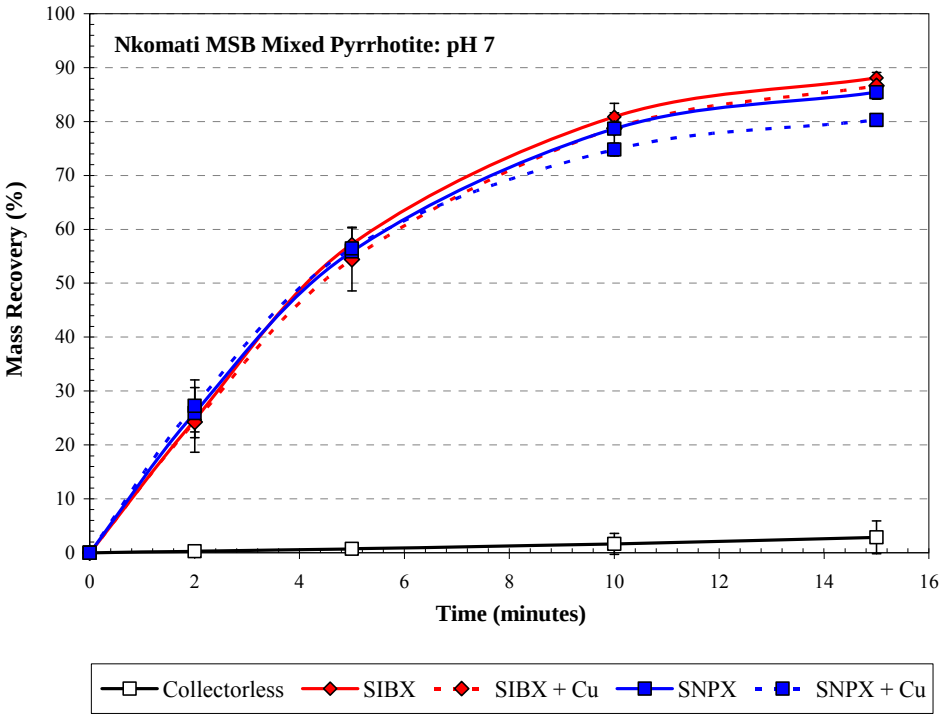

Figure 6.5: Mass recovery versus time from microflotation tests of Nkomati MSB mixed pyrrhotite at pH 7. The 2σ standard deviation is also shown.

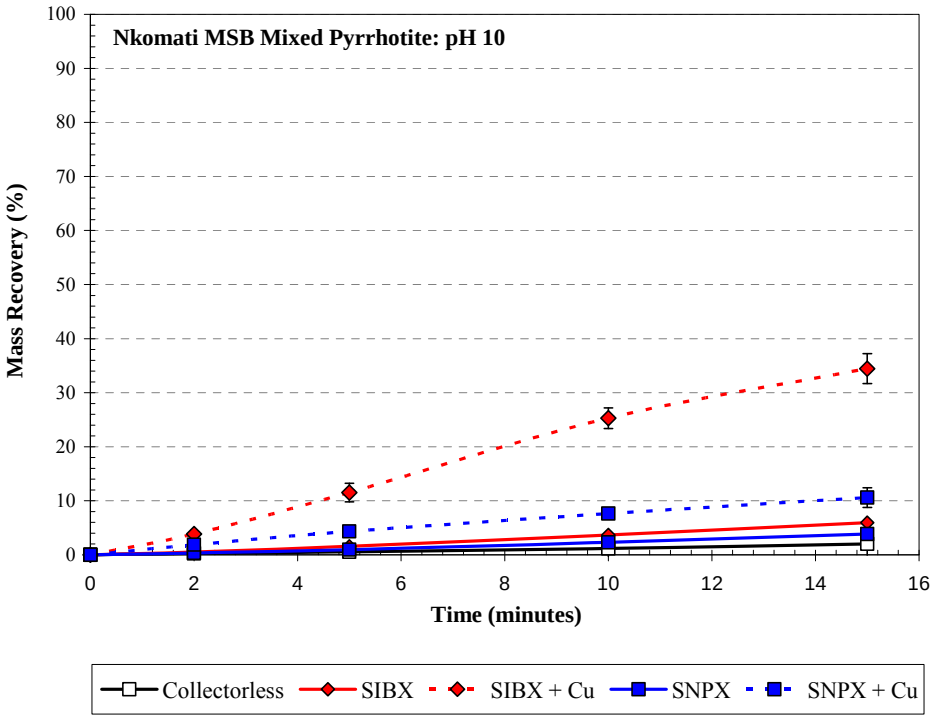

Figure 6.6: Mass recovery versus time from microflotation tests of Nkomati MSB mixed pyrrhotite at pH 10. The 2σ standard deviation is also shown.

6.4 Phoenix Pyrrhotite

Phoenix magnetic pyrrhotite showed poor collectorless floatability at pH 7 as illustrated in figure 6.7, where the final mass recovery obtained in microflotation tests was only 6.15%. The addition of collector had a marked effect on flotation performance both in terms of flotation kinetics and of the final recovery (> 50 % recovery). A higher mass recovery of 66.3 % was obtained for the longer chain length SIBX collector in comparison to the slightly shorter chain length SNPX collector where the recovery was only 51.8 %. The effect of copper activation was mixed, and only had a positive influence on flotation recovery when used in conjunction with SNPX where the recovery increased to 70.3 %.

The increase in pH up to 10 during flotation caused Phoenix magnetic pyrrhotite to have even poorer natural floatability than at pH 7 due to the increase in hydroxide ion concentration, as can be observed in figure 6.8. At pH 10, the final mass recovery of pyrrhotite was only 2.71 %. The addition of collector at this pH did not improve the flotation recovery of pyrrhotite since the maximum flotation recovery for both SIBX and SNPX collectors was less than 10 %. The effect of copper activation however was most apparent and caused a rapid increase in flotation kinetics (recovery of between 30 and 50 % within the first 5 minutes of flotation). The final pyrrhotite recovery obtained for the copper activation tests was greater when SIBX (83.8% recovery) was used as collector relative to SNPX (42.7% recovery).

The calculated pyrrhotite recovery of Phoenix pyrrhotite for selected flotation tests is shown in table 6.1. For the test conditions examined, the calculated pyrrhotite recovery was almost identical to the mass recovery indicating that the final mass recovery is a suitable indicator of Phoenix pyrrhotite flotation performance. It is also evident from table 6.1 that pentlandite recovery was ~ 7 % higher than the mass or calculated pyrrhotite recovery. Since the final pentlandite grade of the concentrates was less than 1.5 wt %, the proportion of pentlandite diluting the concentrate was relatively negligible. Based on the pentlandite liberation shown in figure 6.4, it is more than likely that the majority of the pentlandite recovered was locked flame pentlandite in association with pyrrhotite.

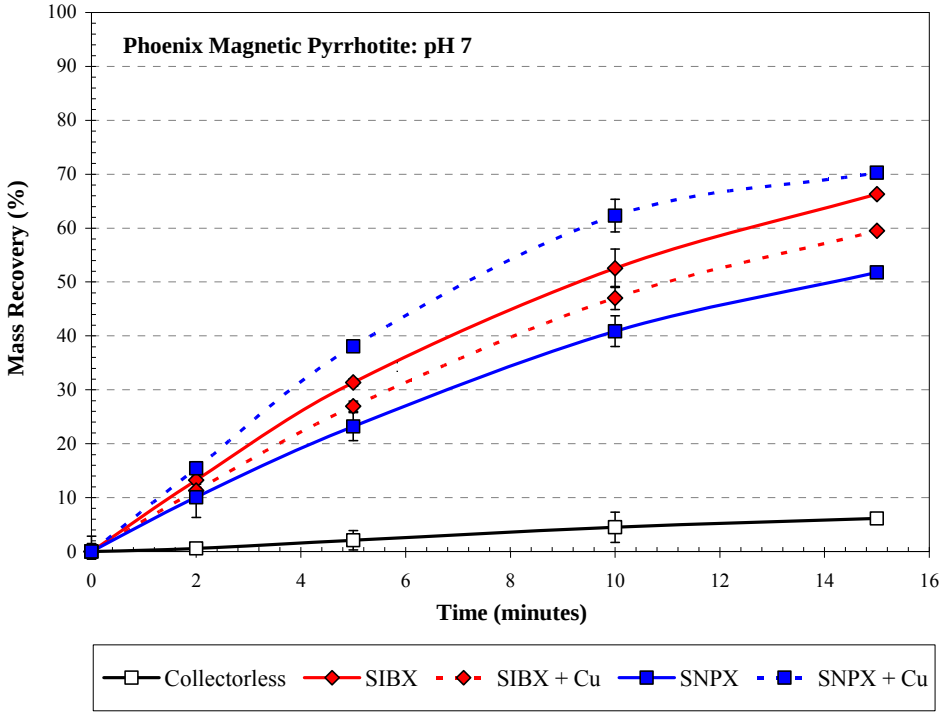

Figure 6.7: Mass recovery versus time from microflotation tests of Phoenix magnetic pyrrhotite at pH 7. The 2σ standard deviation is also shown.

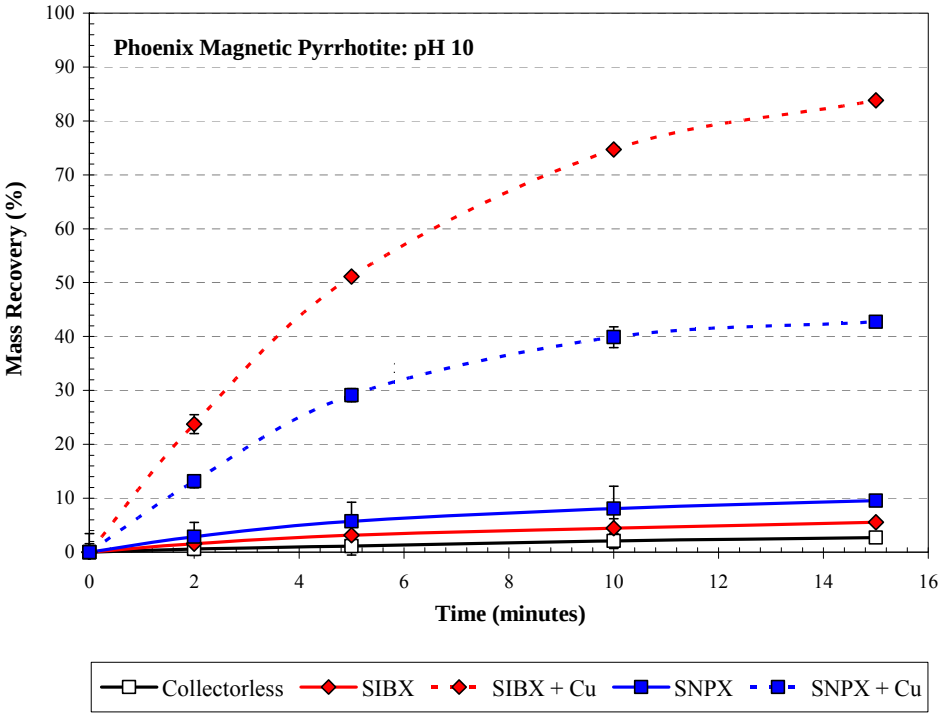

Figure 6.8: Mass recovery versus time from microflotation tests of Phoenix magnetic pyrrhotite at pH 10. The 2σ standard deviation is also shown.

6.5 Sudbury Copper Cliff North Pyrrhotite

Sudbury Copper Cliff North non-magnetic pyrrhotite showed moderate collectorless floatability at pH 7 as shown in figure 6.9. The final pyrrhotite recovery obtained under these conditions was 36.1 % and it is notable that a linear relationship appears to exist between pyrrhotite recovery and time. Pyrrhotite recovery was improved with the addition of SNPX (51.6 % recovery) and even more so with SIBX addition (68.6 % recovery). Unlike the linear relationship observed between pyrrhotite recovery and time for the collectorless flotation test, the addition of copper in conjunction with collector caused a distinct improvement in flotation kinetics where the typical exponential shaped recovery versus time curve was observed.

The flotation results of Sudbury CCN at pH 10 are shown in figure 6.10 where it is evident that the final pyrrhotite mass recovery of ~ 36 % obtained with collector addition was only slightly improved relative to the collectorless flotation test where 27.0 % recovery was obtained. The addition of copper in conjunction with SNPX collector caused further improvement in pyrrhotite floatability (54.5 % recovery) and even more so for the SIBX collector (79.8 % recovery).

The calculated pyrrhotite recovery for the flotation tests of Sudbury CCN pyrrhotite given in table 6.1 was between 5 and 10 % higher than the mass recovery. Similarly, the pentlandite recovery was on the order of ~ 15 % higher than the mass recovery which suggests that pentlandite recovery is significant. However, even though pentlandite recovery was significant, it did negatively affect the grade of pyrrhotite in the concentrate since the maximum pentlandite grade obtained was only 0.61 wt %. Therefore, final mass recovery can be accepted as a suitable indicator of pyrrhotite flotation performance (Table 6.1).

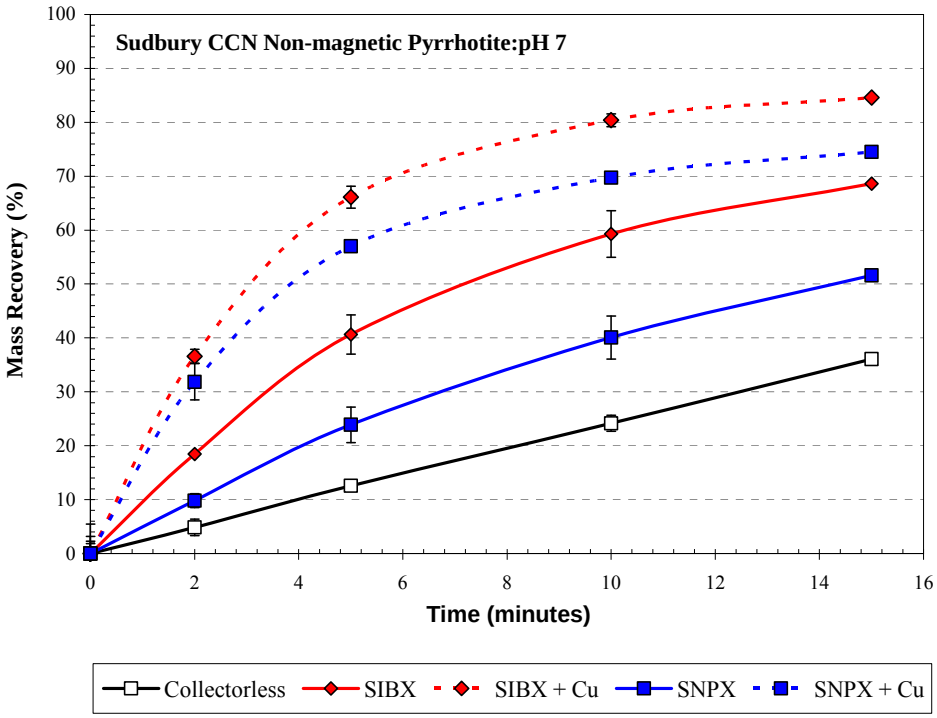

Figure 6.9: Mass recovery versus time from microflotation tests of Sudbury CCN non-magnetic pyrrhotite at pH 7. The 2σ standard deviation is also shown.

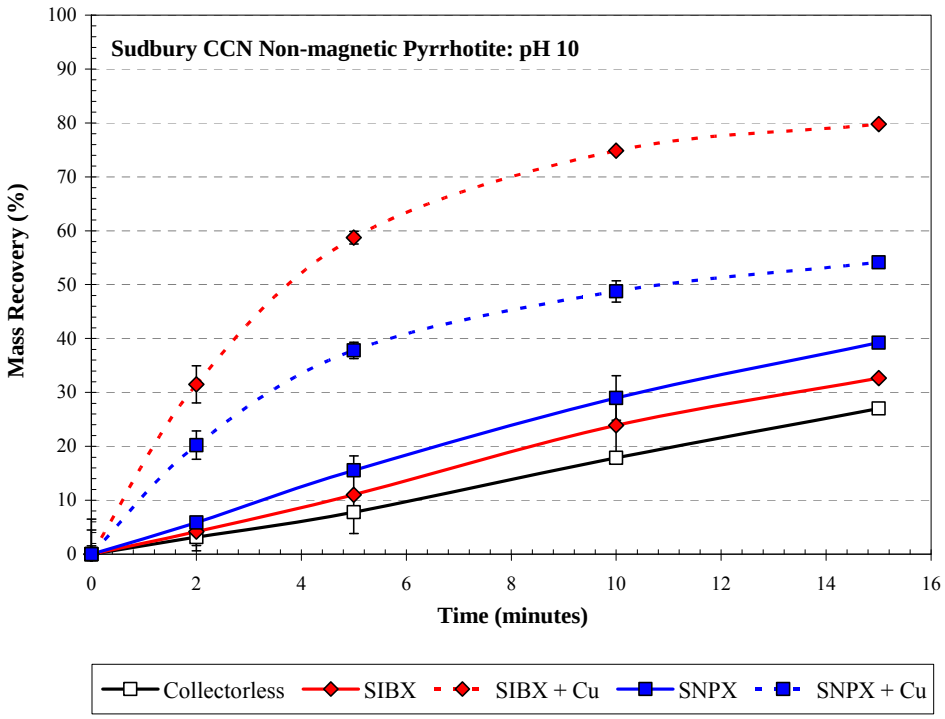

Figure 6.10: Mass recovery versus time from microflotation tests of Sudbury CCN non-magnetic pyrrhotite at pH 10. The 2σ standard deviation is also shown.

6.6 Sudbury Gertrude and Gertrude West Pyrrhotite

The natural floatability of Sudbury Gertrude magnetic pyrrhotite at pH 7 tended to be very poor as can be observed in figure 6.11, where the final mass recovery obtained was only 4.79 %. The addition of reagents (collector ± copper) appeared to have relatively limited effect on the floatability of the Gertrude pyrrhotite. Even the addition of the stronger SIBX collector with copper activation caused only a minor improvement in floatability (32.8 % recovery). In order to confirm that the Gertrude pyrrhotite had not been unduly oxidised during sample preparation a new Gertrude sample was sourced and prepared, namely Gertrude West pyrrhotite. The flotation results of the new Gertrude West pyrrhotite shown in figure 6.12 were remarkably similar to that of the Gertrude pyrrhotite at pH 7. Poor natural floatability was also observed for Gertrude West pyrrhotite (1.36 % recovery). The addition of reagents however, did cause some minor improvement in pyrrhotite floatability. The addition of copper only caused a very slight improvement in pyrrhotite floatability when used in conjunction with SNPX and SIBX (increase from 14.7 to 21.9 %, and 28.4 to 41.8 % recovery respectively).

For both the Gertrude and Gertrude West pyrrhotite samples, collectorless pyrrhotite flotation was very poor at pH 10 as is shown in figures 6.13 and 6.14, respectively. For both these pyrrhotite samples, the flotation recovery even for tests with reagent addition was less than 7 %. The only exception however, occurred for the Gertrude pyrrhotite for which the addition of both SIBX and copper caused an improvement in flotation recovery up to 17.4 %.

Due to the poor floatability of the Gertrude and Gertrude West pyrrhotite under all the test conditions investigated, very low masses were recovered and therefore detailed chemical assays were not possible. The pyrrhotite recovery could only be calculated for the flotation test of the Gertrude West pyrrhotite at pH 7 with SIBX and copper activation. The calculated pyrrhotite recovery for this particular test was 38.8 % which was slightly lower than the actual mass recovery 41.8 %, but most likely within the error of the analysis. However, it is evident from table 6.1 that the pentlandite recovery could be up to double that of the mass recovery. Since the final pentlandite grade varied between 19 and 30 wt %, it can be concluded that the poor flotation performance of the Gertrude and Gertrude West pyrrhotite was actually even more severe than the mass recovery results shown in figures 6.11 to 6.14 would suggest, since the recovery of pentlandite significantly contributed to the total mass recovery.

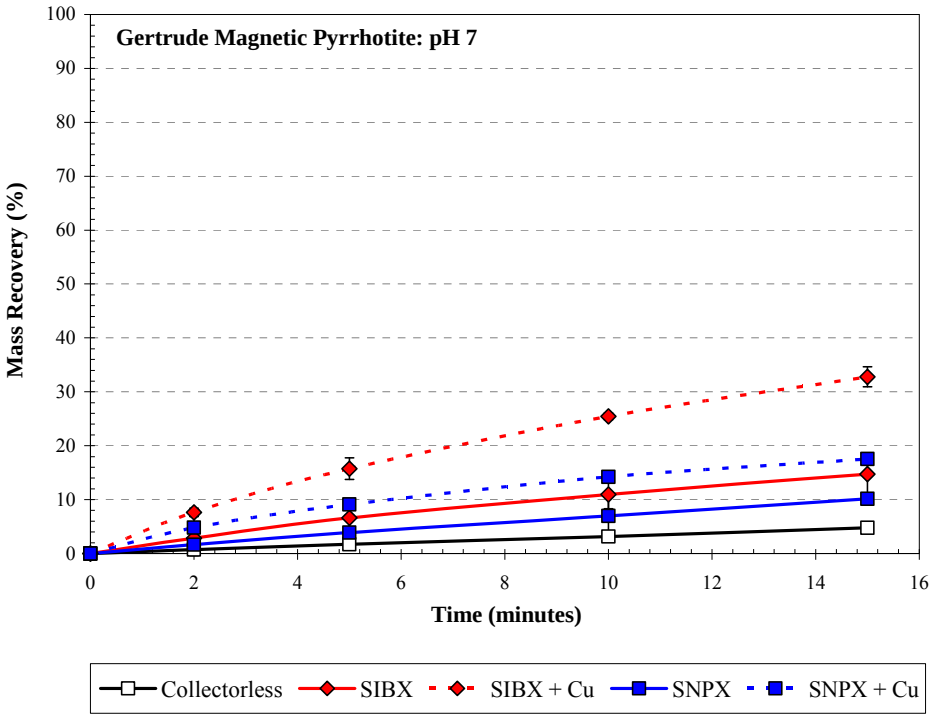

Figure 6.11: Mass recovery versus time from microflotation tests of Sudbury Gertrude magnetic pyrrhotite at pH 7. The 2σ standard deviation is also shown.

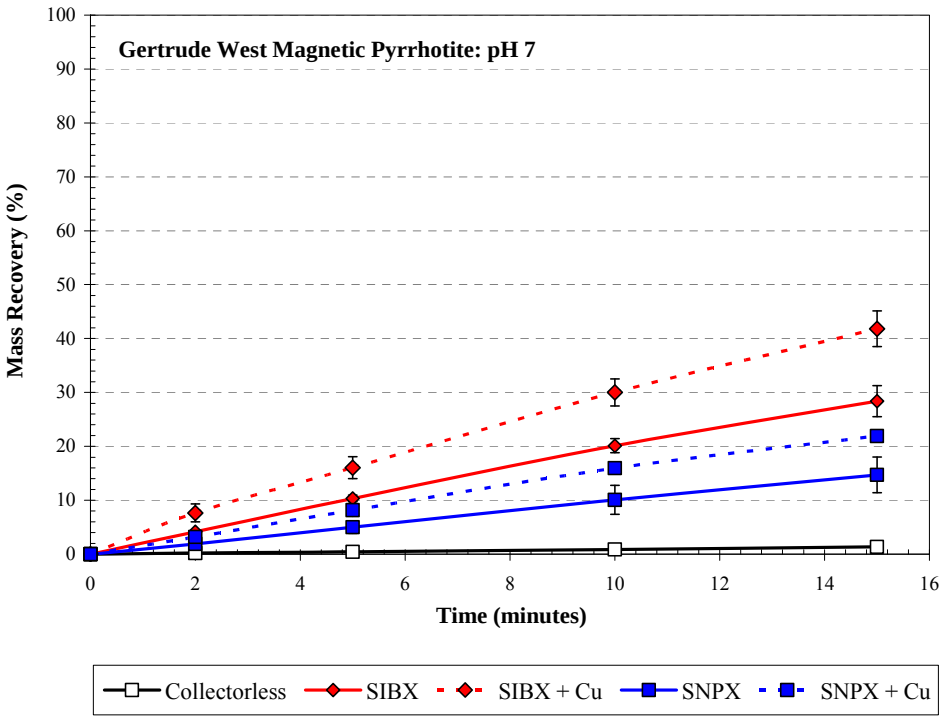

Figure 6.12: Mass recovery versus time from microflotation tests of Sudbury Gertrude West magnetic pyrrhotite at pH 7. The 2σ standard deviation is also shown.

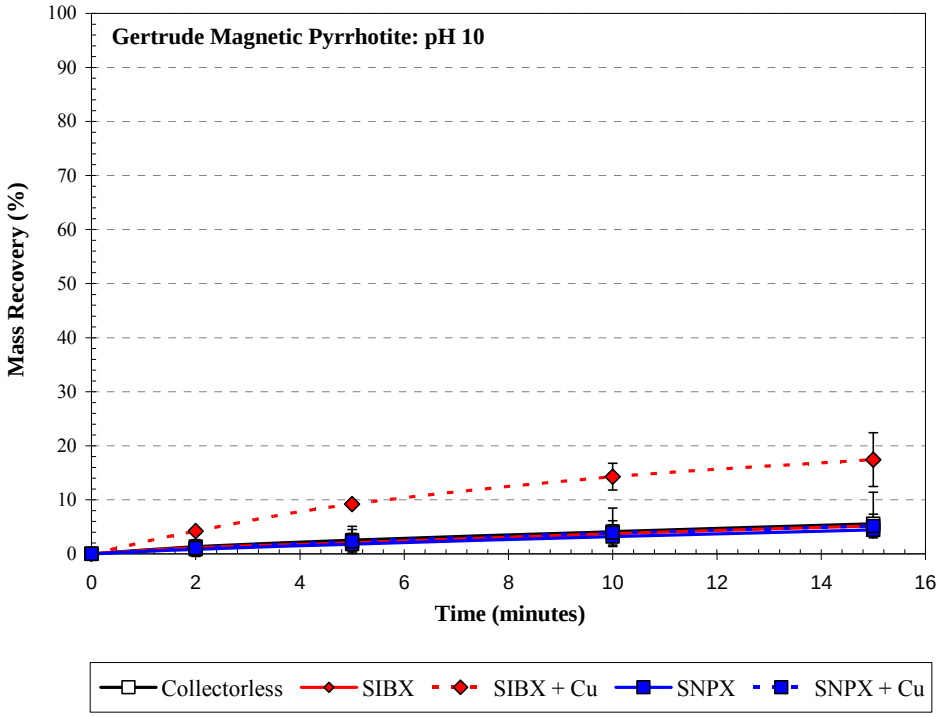

Figure 6.13: Mass recovery versus time from microflotation tests of Sudbury Gertrude magnetic pyrrhotite at pH 10. The 2σ standard deviation is also shown.

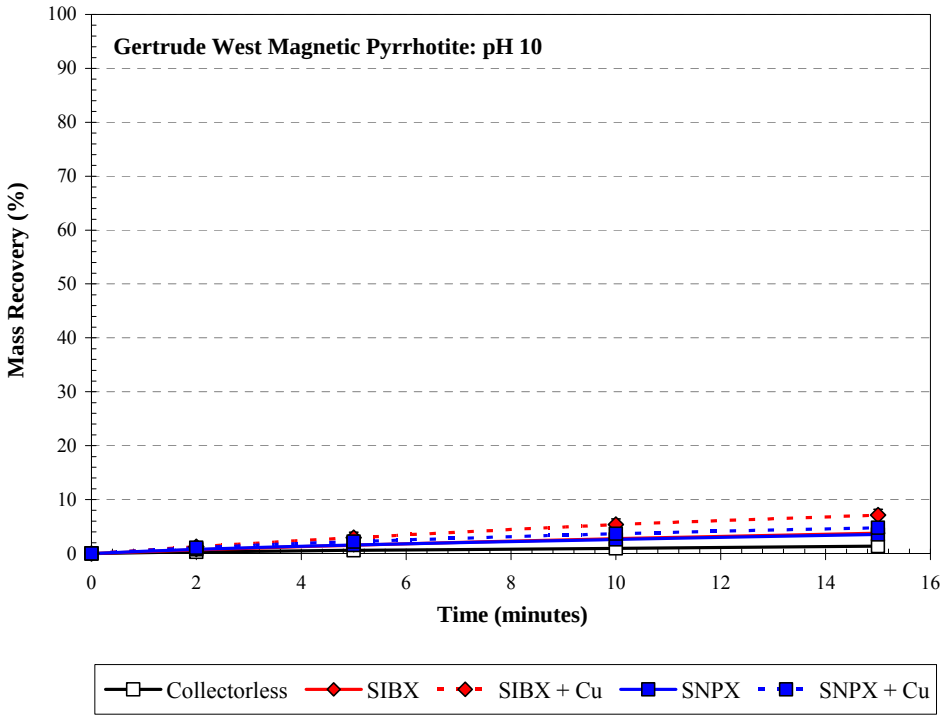

Figure 6.14: Mass recovery versus time from microflotation tests of Sudbury Gertrude West magnetic pyrrhotite at pH 10. The 2σ standard deviation is also shown.

6.7 Comparison of the Floatability of Pyrrhotite Samples

In order to compare the differences in floatability between magnetic, non-magnetic and mixed pyrrhotite samples, the final mass recovery from the different test conditions is shown for comparison in figures 6.15 - 6.18. It is noted that the feed composition of the pyrrhotite samples for the microflotation tests was variably contaminated with additional sulfide minerals such as pentlandite (Figures 6.1 - 6.4) that would have contributed to the mass recovery during flotation. Since the contribution of pentlandite to the mass recovery during the flotation tests has already been examined for the individual pyrrhotite samples (Table 6.1), and shown generally not to be an issue for all samples other than Gertrude and Gertrude West pyrrhotite, further comparisons are performed based on final mass recovery.

Non-magnetic Sudbury CCN pyrrhotite showed the greatest natural floatability or degree of collectorless flotation of all the pyrrhotite samples tested in this study at pH 7 (Figure 6.15). In comparison to the collectorless flotation recovery of the magnetic pyrrhotite and mixed pyrrhotite samples (Sudbury Gertrude and Gertrude West, Phoenix and Nkomati MSB, respectively), the 36.1 % mass recovery obtained for the Sudbury CCN non-magnetic pyrrhotite was by far the greatest. No consistent relationship between the natural flotation recovery of magnetic and mixed pyrrhotite samples can be observed from figure 6.15. This suggests that none of them showed preferentially greater natural floatability to the other (< 6.15 % recovery).

With the addition of SIBX collector to the flotation system at pH 7, the floatability of all the pyrrhotite samples showed a dramatic increase as evidenced by the high total mass recovery of pyrrhotite (Figure 6.15). The final mass recovery of Sudbury CCN non-magnetic and Phoenix magnetic pyrrhotite was fairly similar (~ 67 % recovery), whereas the Nkomati mixed pyrrhotite was the most floatable (88 % recovery). Both the magnetic Sudbury Gertrude and Gertrude West pyrrhotite samples showed very poor mass recovery during flotation, even with the addition of SIBX collector (< 28 % recovery). Based on the contribution of pentlandite to the mass recovery in the Gertrude and Gertrude West samples during flotation (Section 6.4), it can be surmised that the poor floatability of this pyrrhotite was even more severe than the mass recovery would suggest.

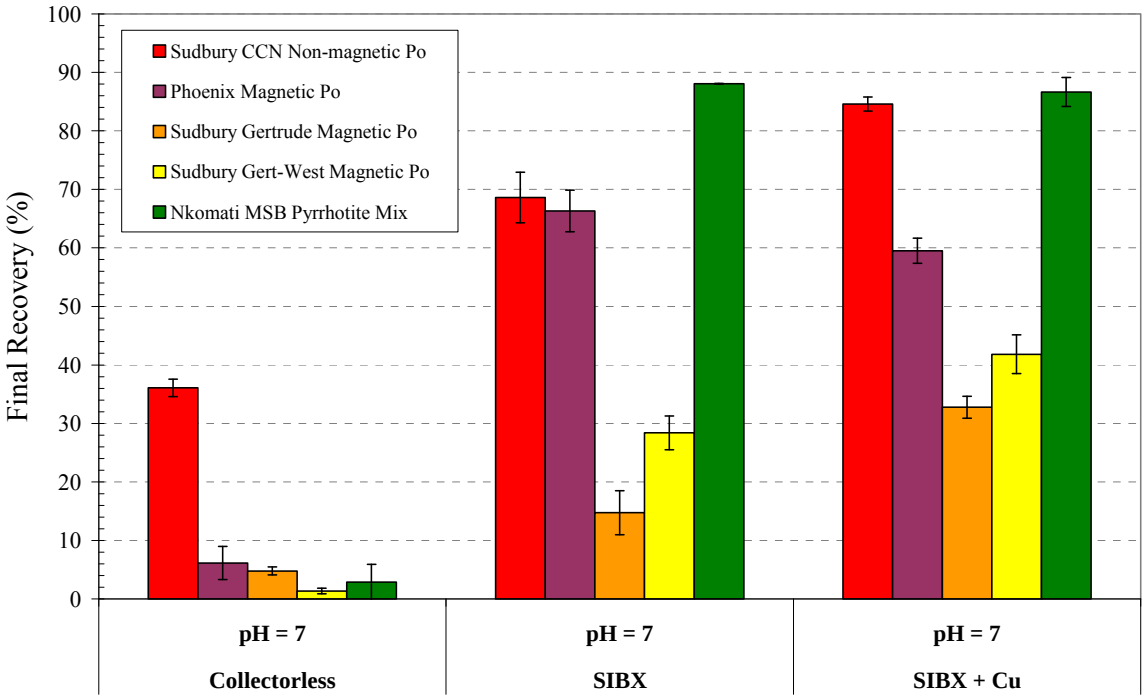

Figure 6.15: Comparison of the final flotation mass recovery for all pyrrhotite samples at pH 7 shown for SIBX collector tests. The 2σ standard deviation is also shown.

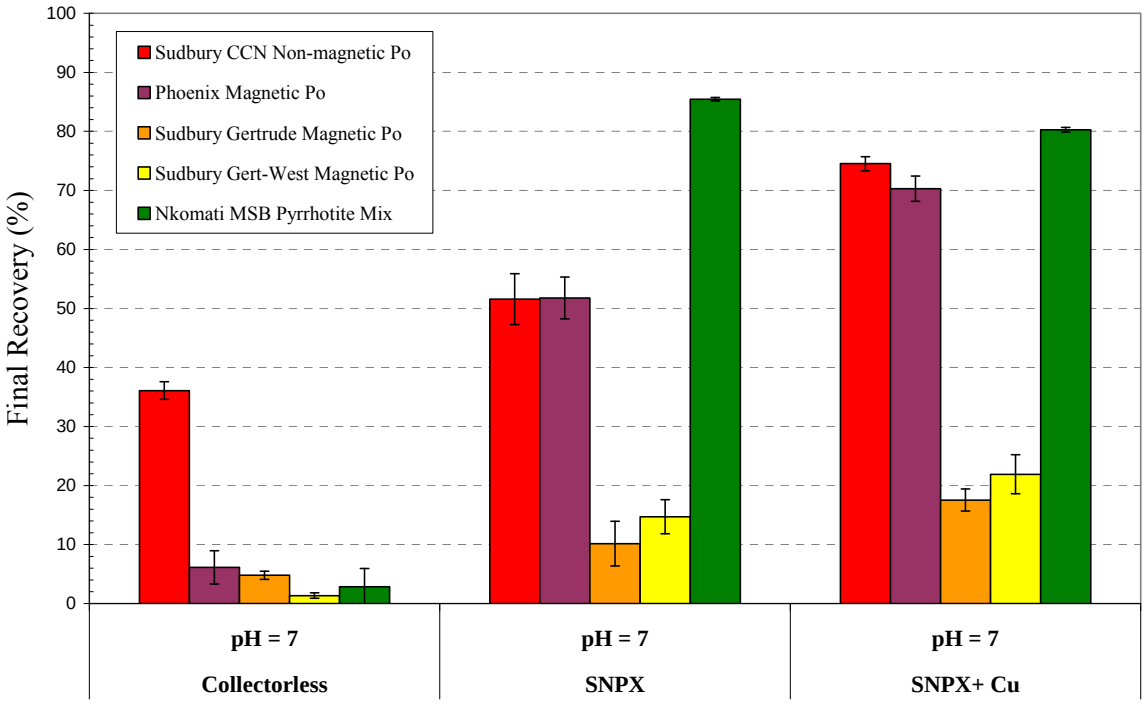

Figure 6.16: Comparison of the final flotation mass recovery for all pyrrhotite samples at pH 7 shown for SNPX collector tests. The 2σ standard deviation is also shown.

The addition of the slightly shorter chain length SNPX collector to the flotation system at pH 7 caused similar changes in floatability for the pyrrhotite samples as SIBX, although the effects were not quite so dramatic (Figure 6.16). For example, the addition of SIBX caused an increase in flotation recovery of Sudbury CCN non-magnetic pyrrhotite from 31% recovery (collectorless flotation), to 68.6 %, whereas the addition of SNPX only caused an increase up to 51.6 % recovery.

The effect of copper activation on pyrrhotite floatability in conjunction with the addition of SIBX collector for all the pyrrhotite samples at pH 7 shown in figure 6.15 was quite variable. Some pyrrhotite samples showed increased floatability or improved recovery (Sudbury CCN, Sudbury Gertrude and Gertrude West), whereas others showed negligible improvement (Phoenix, Nkomati MSB). The effect of copper activation on pyrrhotite floatability with the addition of SNPX collector was generally similar to the tests with SIBX collector (Figure 6.16). However, it is noted that the Phoenix magnetic pyrrhotite showed a distinct improvement in flotation performance when copper activation occurred in the presence of SNPX collector.

The collectorless flotation recovery of all the pyrrhotite samples at pH 10 is shown in figure 6.17, and it is evident that the floatability is lower than at pH 7. The non-magnetic Sudbury CCN pyrrhotite sample was still the most floatable of all the pyrrhotite samples as evidenced by its good natural floatability (27.0 % recovery) relative to the other magnetic pyrrhotite and mixed pyrrhotite samples (< 5.5 % recovery). The addition of either SIBX or SNPX at pH 10 served to only significantly improve the floatability of the non-magnetic Sudbury CCN pyrrhotite, whereas the addition of collector in conjunction with copper influenced the floatability of all the pyrrhotite samples (Figures 6.17, 6.18). The recovery of non-magnetic Sudbury CCN pyrrhotite increased from 32.6 to 79.8 % with copper activation, magnetic Phoenix pyrrhotite increased from 5.54 to 83.8 % with copper activation and the mixed Nkomati pyrrhotite recovery increased from 5.93 to 34.5%. Even the magnetic Gertrude and Gertrude West pyrrhotite sample showed some minor improvement in flotation recovery e.g. increase from 5.17 to 17.4 % recovery for Gertrude pyrrhotite. It is also noted that the effect of copper activation was far greater for the longer chain length SIBX collector than the shorter SNPX collector. The flotation recovery showed an almost two fold increase for SIBX relative to the small increase in floatability evidenced for the SNPX collector (e.g. increase from 39.2 to 54.2 % recovery for non-magnetic Sudbury CCN pyrrhotite).

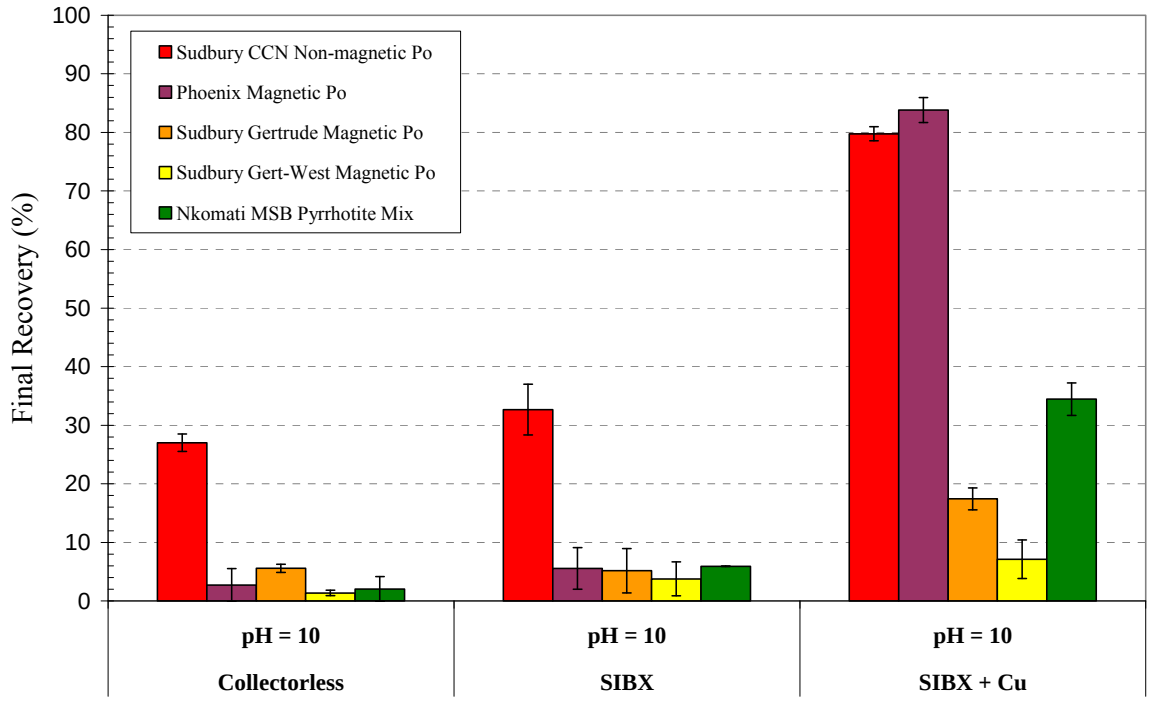

Figure 6. 17: Comparison of the final flotation mass recovery for all pyrrhotite samples at pH 10 shown for SIBX collector tests. The 2σ standard deviation is also shown.

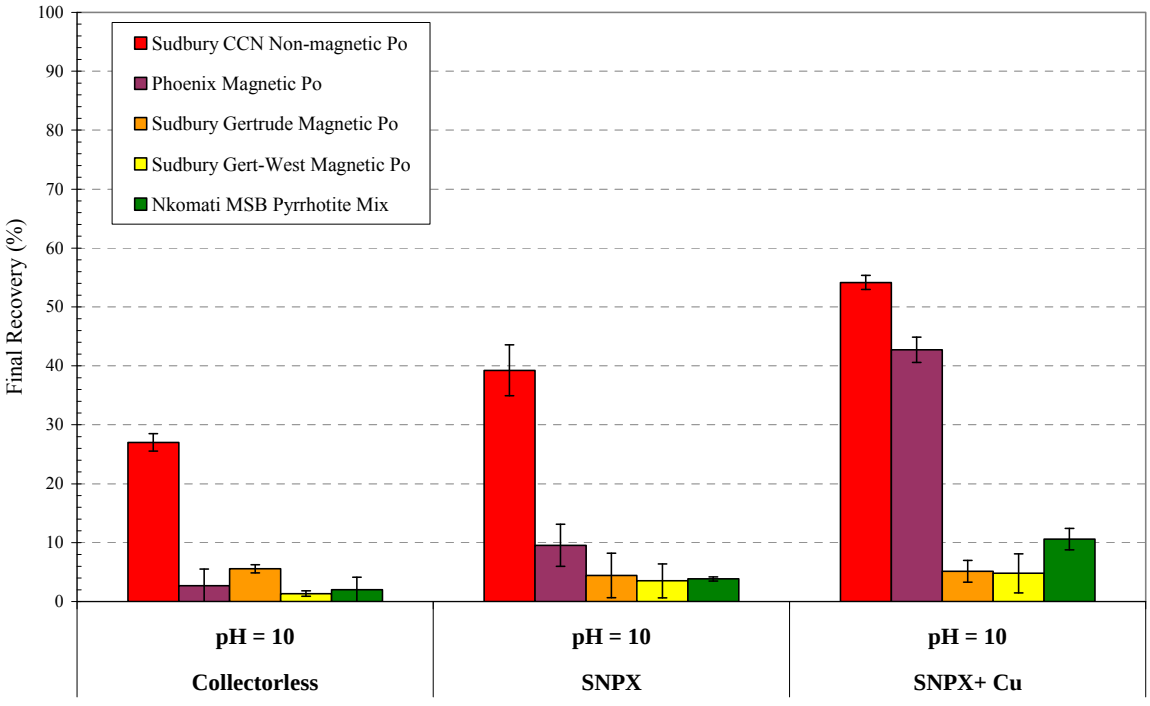

Figure 6.18: Comparison of the final flotation mass recovery for all pyrrhotite samples at pH 10 shown for SNPX collector tests. The 2σ standard deviation is also shown.

6.8 Key findings

Key features noted with respect to the microflotation of pyrrhotite from selected nickel and platinum group element ore deposits were as follows:

MLA analysis of the feed samples prepared for microflotation tests of the Nkomati MSB mixed pyrrhotite, Phoenix magnetic pyrrhotite, Sudbury CCN non-magnetic pyrrhotite, Sudbury Gertrude and Gertrude West magnetic pyrrhotite showed that all samples were comprised of greater than 75 wt % pyrrhotite and greater than 84 wt % sulphides. Pyrrhotite liberation was noted to be quite variable, Sudbury CCN non-magnetic pyrrhotite and Sudbury Gertrude West magnetic pyrrhotite were over 90 % liberated, Nkomati MSB pyrrhotite was 88.4 % liberated whereas the Phoenix magnetic pyrrhotite was only 50.7 % liberated. The lower pyrrhotite liberation in the Nkomati and Phoenix pyrrhotite flotation feed samples was due to the presence of locked flame pentlandite. Pentlandite liberation for these two pyrrhotite samples was only ~ 50 % compared to Sudbury CCN and Sudbury Gertrude West pentlandite that was greater than 77 % liberated.

The collectorless flotation for all pyrrhotite samples was observed to be greater at pH 7 instead of pH 10 e.g. the Phoenix magnetic pyrrhotite showed a decrease in collectorless flotation recovery from 6.15 to 2.71 % with an increase in pH.

The flotation recovery for all pyrrhotite samples increased with the addition of collector at pH 7 e.g. the Phoenix magnetic pyrrhotite showed an increase in flotation recovery from 6.15 to 51.8 wt % with the addition of SNPX collector at pH 7. Sudbury CCN non-magnetic pyrrhotite was the only pyrrhotite sample to show a significant increase in flotation recovery with the addition of collector at pH 10. e.g. increase in flotation recovery from 27.0 to 39.2 wt % with the addition of SNPX collector. The flotation recovery was generally greater for the longer chain length SIBX collector relative to SNPX collector due to the increased hydrophobicity of SIBX relative to SNPX.

In general, the flotation recovery of the pyrrhotite samples increased with copper activation, but was heavily influenced by pyrrhotite mineralogy, pH and collector chain length. Nearly all pyrrhotite samples other than the Nkomati MSB mixed pyrrhotite showed an increase in flotation recovery due to copper activation at pH 7, but it was noted that the results were

more consistent for copper activation in conjunction with the shorter chain length SNPX collector e.g. the Phoenix magnetic pyrrhotite showed an increase in flotation recovery from 51.8 to 70.3 wt % due to copper activation in conjunction with SNPX addition at pH 7. At pH 10, some pyrrhotite samples showed an increase in flotation recovery due to copper activation, but only for the longer chain length SIBX collector. Only those pyrrhotite samples that already had improved floatability due to SNPX addition were positively affected by copper activation e.g. the Phoenix magnetic pyrrhotite showed an increase in flotation recovery from 9.56 to 42.7 wt % due to copper activation in conjunction with SNPX addition at pH 10.

The Sudbury CCN non-magnetic pyrrhotite showed the greatest collectorless flotation recovery at pH 7 and 10 (36.1 and 27.0 % recovery) compared to the other pyrrhotite samples. No significant differences were observed between the collectorless flotation recovery of the other magnetic and mixed pyrrhotite samples at pH 7 or 10 (< 6.15 % recovery). The addition of reagents at pH 7 caused a marked influence in the flotation recovery of the non-magnetic Sudbury CCN, magnetic Phoenix and mixed Nkomati MSB pyrrhotite samples (e.g. up to 88.1 % recovery for Nkomati MSB mixed pyrrhotite at pH 7 with SIBX addition). The addition of reagents at pH 10 however, only caused a marked influence in the flotation recovery for the Sudbury CCN non-magnetic and Phoenix magnetic pyrrhotite. The magnetic Sudbury Gertrude and Gertrude West pyrrhotite samples showed the poorest overall flotation recovery of all the pyrrhotite samples examined with reagent addition; where the maximum recovery obtained for the Sudbury Gertrude West pyrrhotite sample was only 41.8 % with copper activation in conjunction with SIBX addition at pH 7.